TECHNICAL REPORT STANDARD TITLE PAGE

1. Report No.	2. Government Accession No.	3. Recipient's Catalog No.
FHWA/TX-83/9+247-5F		

4. Title and Subtitle	5. Report Date
FATIGUE BEHAVIOR OF LONGITUDINAL TRANSVERSE STIFFENER INTERSECTION	May 1983
	6. Performing Organization Code

7. Author(s)	8. Performing Organization Report No.
John D. Pass, Karl H. Frank, and Joseph A. Yura	Research Report 247-5F

9. Performing Organization Name and Address	10. Work Unit No.
Center for Transportation Research The University of Texas at Austin Austin, Texas 78712-1075	11. Contract or Grant No. Research Study 3-5-79-247
	13. Type of Report and Period Covered
12. Sponsoring Agency Name and Address Texas State Department of Highways and Public Transportation; Transportation Planning Division P. O. Box 5051 Austin, Texas 78763	Final
	14. Sponsoring Agency Code

15. Supplementary Notes

Study conducted in cooperation with the U. S. Department of Transportation, Federal Highway Administration. Research Study Title: "Estimation of the Fatigue Life of Structural Steel Bridge Details"

16. Abstract

The fatigue performance of a twin girder steel bridge in Dallas was investigated in this project. The fatigue life of the bridge was estimated using the results of field tests to determine the bridge's response to traffic loads and analytical and experimental studies to determine the fatigue performance of the structural details on the bridge. These studies indicated that the bridge's fatigue life was controlled by the detail used at the intersection of the longitudinal transverse stiffener. This final report presents the results of an experimental fatigue study of this detail and tests upon a retrofit detail designed to improve the fatigue life of the bridge. The experimental fatigue results confirmed the analytically estimated poor fatigue performance of this detail. The results indicate that the retrofit detail will increase the fatigue life of the bridge by a factor of at least two.

17. Key Words	18. Distribution Statement
fatigue behavior, twin girder steel bridge, field tests, traffic loads, intersection, longitudinal stiffener, transverse stiffener, retrofit	No restrictions. This document is available to the public through the National Technical Information Service, Springfield, Virginia 22161.

19. Security Classif. (of this report)	20. Security Classif. (of this page)	21. No. of Pages	22. Price
Unclassified	Unclassified	100	

Form DOT F 1700.7 (8-69)

FATIGUE BEHAVIOR OF LONGITUDINAL TRANSVERSE STIFFENER INTERSECTION

by

John D. Pass
Karl H. Frank
and
Joseph A. Yura

Research Report No. 247-5F

Research Project No. 3-5-79-247

Evaluation of the Fatigue Life of Structural Steel Bridge Details

Conducted for

Texas

State Department of Highways and Public Transportation

In Cooperation with the
U.S. Department of Transportation
Federal Highway Administration

by

CENTER FOR TRANSPORTATION RESEARCH
BUREAU OF ENGINEERING RESEARCH
THE UNIVERSITY OF TEXAS AT AUSTIN

May 1983

The contents of this report reflect the views of the authors who are responsible for the facts and accuracy of the data presented herein. The contents do not necessarily reflect the views or policies of the Federal Highway Administration. This report does not constitute a standard, specification or regulation.

There was no invention or discovery conceived or first actually reduced to practice in the course of or under this contract, including any art, method, process, machine, manufacture, design or composition of matter, or any new and useful improvement thereof, or any variety of plant which is or may be patentable under the patent laws of the United States of America or any foreign country.

PREFACE

This is the final report on Research Project 3-5-79-247 entitled "Evaluation of the Fatigue Life of Structural Steel Bridge Details." The study described was conducted as a part of the overall research program at The University of Texas at Austin, Center for Transportation Research. The work was sponsored jointly by the Texas Department of Highways and Public Transportation and the Federal Highway Administration.

Sincere thanks are due various support personnel of the Phil M. Ferguson Structural Engineering Laboratory. Mr. Richard Marshall and Mr. Dan Perez supervised and assisted in the building and maintenance of electronic data acquisition equipment used in the field tests. Mrs. Laurie Golding aided in the purchasing of the many items required for field testing. Mr. Gorham Hinckley and Mr. George Moden helped in setting up and running the laboratory fatigue test. Mrs. Sandi Provot and Ms. Patricia Henderson carefully typed the manuscript.

Mr. Frank Endres developed the computer software used to reduce the large amounts of field test data.

Special thanks are given to Research Assistants Antonio Leite, Ashok Gupta, David Platten, and Peter Hoadley for their work on the various aspects of the project.

Liaison with the Texas Department of Highways and Public Transportation was maintained through the contact representatives Bob Reed and Gerry Fox. Their cooperation in the field testing was invaluable. Mr. Randy Losch was the contact representative for the Federal Highway Administration.

S U M M A R Y

The fatigue performance of a twin girder steel bridge in Dallas was investigated in this project. The fatigue life of the bridge was estimated using the results of field tests to determine the bridge's response to traffic loads and analytical and experimental studies to determine the fatigue performance of the structural details on the bridge. These studies indicated that the bridge's fatigue life was controlled by the detail used at the intersection of the longitudinal transverse stiffener. This final report presents the results of an experimental fatigue study of this detail and tests upon a retrofit detail designed to improve the fatigue life of the bridge. The experimental fatigue results confirmed the analytically estimated poor fatigue performance of this detail. The results indicate that the retrofit detail will increase the fatigue life of the bridge by a factor of at least two.

I M P L E M E N T A T I O N

The results of this study indicate that the intersection of the longitudinal and transverse stiffener produces an extremely poor fatigue detail. The fatigue life of this detail is lower than the AASHTO fatigue category E'. It is recommended that the bridge studied be retrofitted using the detail given in this report and detailed in Appendix B. Other bridges with similar details should also be retrofitted. New designs should avoid this detail if possible. If the intersection of the stiffeners cannot be avoided, the longitudinal stiffener should be attached to the transverse stiffener using a partial penetration fillet weld designed using the formula in Appendix B. The resulting detail should have a fatigue performance at least equal to the AASHTO fatigue category E.

TABLE OF CONTENTS

Chapter Page

L I S T O F T A B L E S

LIST OF FIGURES

Figure Page

CHAPTER 1

INTRODUCTION

This is the final report of Project 247, "Evaluation of the Fatigue Life of Steel Bridges." The project investigated the expected fatigue performance of a twin girder bridge in Dallas, Texas. The design plans of the bridge were evaluated and a visual inspection of the bridge was performed. The structure was designed before significant changes in the AASHTO fatigue provisions were adopted. Consequently, the bridge did not meet the new fatigue design requirements. The review of the bridge plans and the visual inspection revealed that the bridge contained a weld detail that was not covered in the AASHTO specifications. This detail occurred at the longitudinal-transverse stiffener intersection (LTSI). The behavior of the detail was examined analytically in report 247-1. The results of an experimental fatigue study are presented in this report.

In order to accurately assess the fatigue stresses generated due to traffic in the bridge, a field study of the bridge was undertaken. The stresses due to normal traffic and from a test vehicle were measured. The local stresses in the vicinity of the LTSI detail and at the flange thickness transition butt welds were also investigated. The field test method and general results are given in report 247-2. Report 247-4 is an in-depth fatigue analysis of the recorded stress histories. Report 247-3 contains the results of the analysis of the expected behavior of the flange butt welds.

The results of the field tests and the analytical studies indicated that the flange butt welds would not be subject to fatigue cross growth. The LTSI detail was found to be the critical detail. The fatigue life of the LTSI detail based on the results of the field study and a finite element-fracture mechanics fatigue life study was estimated to be of the order of 50 years. In order to confirm the analytically predicted fatigue behavior, an experimental fatigue study of the LTSI detail was undertaken. The experimental results are presented

in this report. In addition, retrofit procedures for improving the fatigue life of the LTSI detail were investigated. A recommended retrofit procedure is given in Appendix B.

1.1 Fatigue Strength

Fracture of metals occurring below the yield stress after repeated variation in stress is termed fatigue. It is a process whereby small flaws propagate into macroscopic cracks under repeated application of load [1]. The rate of crack growth increases exponentially with an increase in crack size. At some point, the applied stresses on the uncracked area are large enough to cause yielding of the net section or initiation of unstable or brittle crack extension causing failure.

There are many factors such as stress range (S_R), residual stress, material fracture toughness, cyclic frequency, and type of detail, that affect the fatigue strength of structures. The two most important factors are stress range and type of detail [1,2].

The type of detail refers to several factors which include the following:

1) type of weld, for instance, a fillet or a butt weld.

2) geometry of the detail, specifically the relative sizes and areas of the pieces that are welded together.

3) stress concentrations caused by changes in geometry.

4) weld defects such as lack of penetration, porosity, inclusion of slag, undercutting, incomplete fusion, and cracks.

Stress range is defined as the difference between the nominal maximum and minimum stresses at the location of the detail. In effect, this means that only the live load and impact stresses need to be considered.

For bridge design, the American Association of State Highway and Transportation Officials (AASHTO) [3,4] has adopted a set

of stress range-life relationships (S-N curves) for different detail categories as shown in Fig. 1.1. These curves are based on experimental data using a 95% confidence interval for 95% survival. For example, a Category A detail, representing the best fatigue performance, would be a rolled section while a Category E detail, representing a relatively poor fatigue performance, would be represented by an intermittent fillet weld on a plate girder.

Category E' was added in the 1979 Interim Specification to the AASHTO Bridge Specification following the results of tests performed on beams with cover plate details with flange thicknesses greater than 1.25 inches [5]. This addition indicates that there may be other details which are not accurately represented by the present fatigue categories. The design of a particular detail using the wrong stress category may lead to an unsafe or faulty design. In addition, there are some details which have not been tested so the category must be estimated. Of particular concern are any details which are suspected of following the trend of Category E' since these details can fail under very low stress ranges.

1.2 Bridge Details

The structural system of the bridge consists of continuous twin plate girders with intersecting floor beams. The expressway was designed and constructed before the detail categories for fatigue strength were adopted by AASHTO. One particular detail under study occurs on the main girders at the floor beam connections. An elevation of a typical girder is shown in Fig. 1.2. The transverse stiffeners are used to carry the concentrated loads applied by the floor beams and increase the web shear strength. The longitudinal stiffeners are used to increase the out of plane buckling strength of the web by creating a nodal point in the web. Normally,

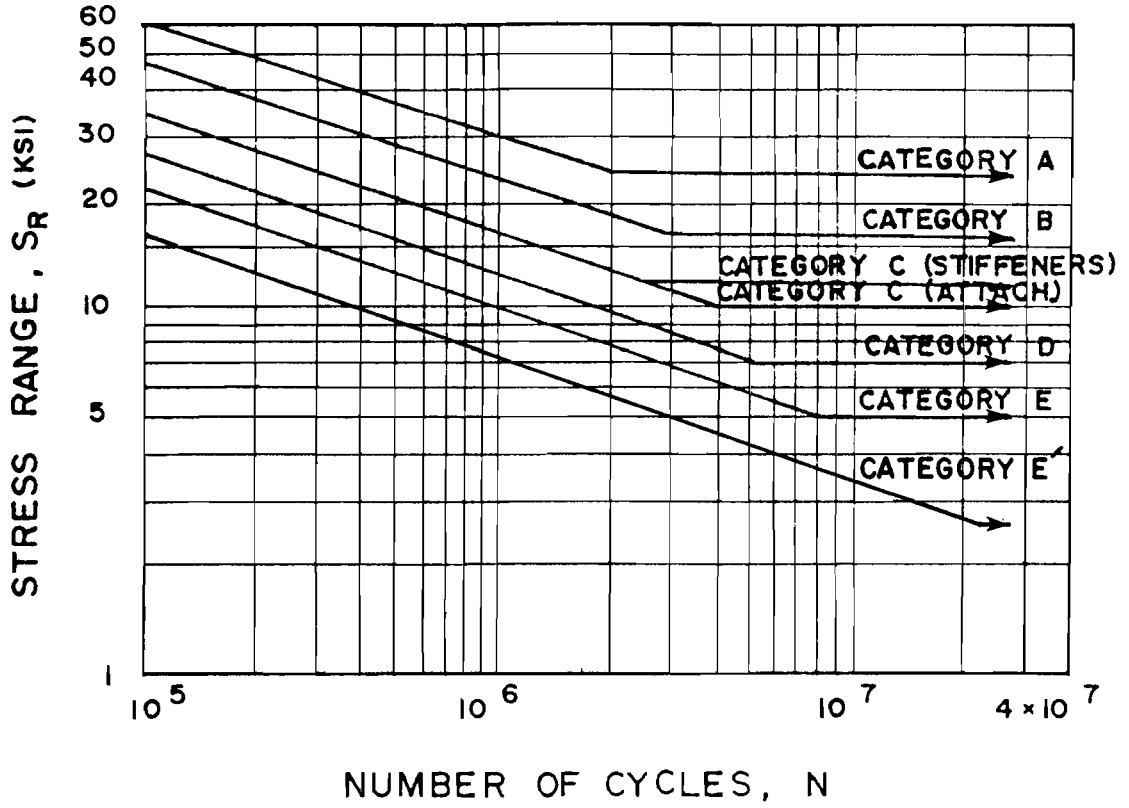

Fig. 1.1 Design S_R-N relationships

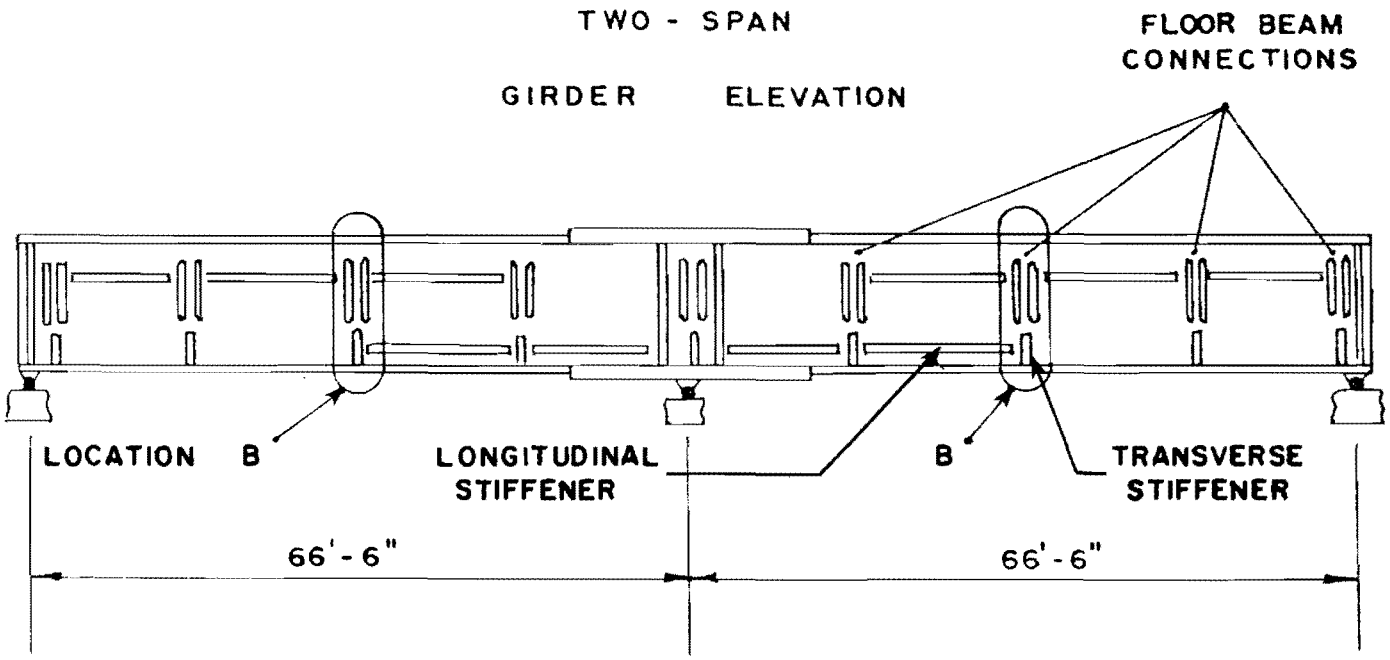

Fig. 1.2 Continuous plate girder

longitudinal stiffeners are located in compressive stress regions which are not fatigue critical areas. Since the expressway is a series of continuous structures, the negative and positive moment regions shift according to the location of the applied load. The resulting stress reversals near inflection points may cause tensile stresses in the bottom flange at locations B in Fig. 1.2.

Fig. 1.3 shows an expanded view of location B in the bridge. Of particular interest is detail "A" at the intersection of the longitudinal and transverse stiffeners. The 1977 AASHTO Specification does not have a fatigue category for stiffener intersections. Section 1.7.43D in the Specification recommends a distance of four to six times the web thickness for the clear distance between the intersection of a transverse stiffener with the weld connecting the flange and web of a plate girder. This is to avoid having excessive stress concentration overlap due to the fillet welds and to help prevent web sidesway bend fatigue problems when the transverse stiffeners are not welded to the tension flange; however, this specification does not apply to stiffener intersections.

Termination of the longitudinal stiffener by itself is a Category E detail while the transverse stiffener by itself is a Category C detail. As can be seen in Fig. 1.3, the total distance between the transverse and longitudinal stiffener is 1/2" - not including the welds which are 5/16". This does not provide any distance between stiffener welds and in effect provides an overlapping weld area. The close proximity of the weld toes of the two stiffeners can cause the two stress concentration fields to overlap producing higher stress concentrations. It appears obvious that at best the detail involved would be a Category E; however, it is not clear as to how large a gap between the two stiffeners is needed in order to provide this Category. The gap width is restricted by local web buckling which can occur in the unstiffened gap region between the longitudinal and transverse stiffeners.

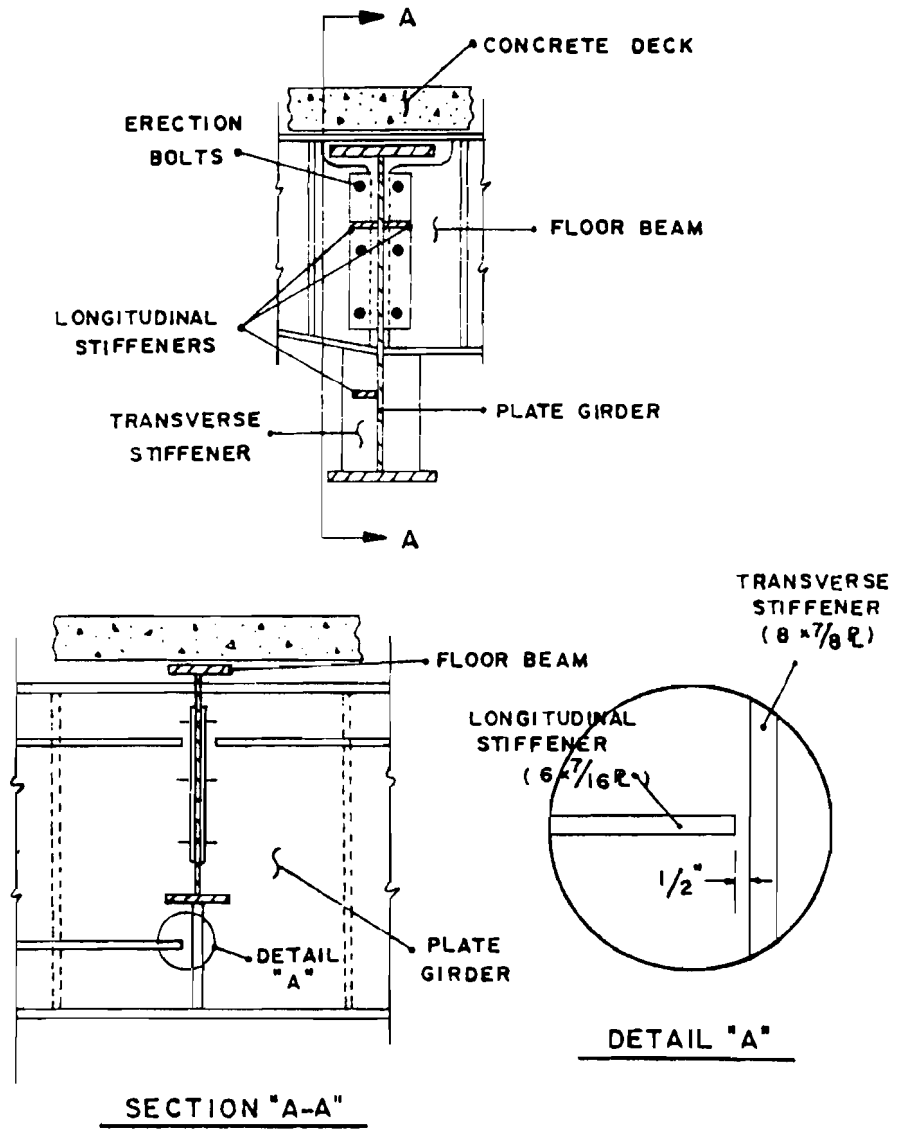

Fig. 1.3 Bridge details at location "B"

1.3 Previous Work

A finite element analysis of the stiffener intersection detail was performed by Platten [6]. The geometry of the detail was varied to determine the stress concentration factor at the weld toe, K_t, and fracture mechanics principles were used to estimate the fatigue lives of the details. For the actual bridge detail, Platten estimated that the S_R-N relationship would be considerably less than that given by Categories E or E' as shown in Fig. 1.4. Platten determined K_t for other cases in which girder web thickness, longitudinal stiffener width, longitudinal stiffener thickness, and gap length at the stiffener intersection were varied. Using his results, Platten developed a relationship between the area of the longitudinal stiffener, A_{st}, divided by the thickness of the girder web, t_w. As the ratio A_{st}/t_w increased, so did K_t. This linear relationship can be seen in Fig. 1.5. His results pertaining to the influence of gap length upon K_t show that as gap size increased from 1/2" to 2", K_t decreased by 38%.

1.4 Purpose and Scope

The purpose of the research performed was three fold. First, to develop an experimental S_R-N curve as a lower bound to the fatigue life of the stiffener intersection shown in Fig. 1.3 for comparison with Platten's predictions. Second, to experimentally determine the effects of changing detail geometry on fatigue life to compare with Platten's theoretical analysis. Third, to develop a practical method to improve the fatigue life of the existing detail, called a retrofit, in case the fatigue life of the bridge, which is being evaluated by others using the actual loading history, is less than desired.

A series of 14 fatigue specimens and tests were planned. Ten fatigue tests are performed to develop the S_R-N curve while also determining the effects of geometry change on the fatigue life. The remaining four specimens are used to develop retrofit procedures to improve the fatigue life of detail. Three different specimen geometries were used in which the longitudinal stiffener size and gap

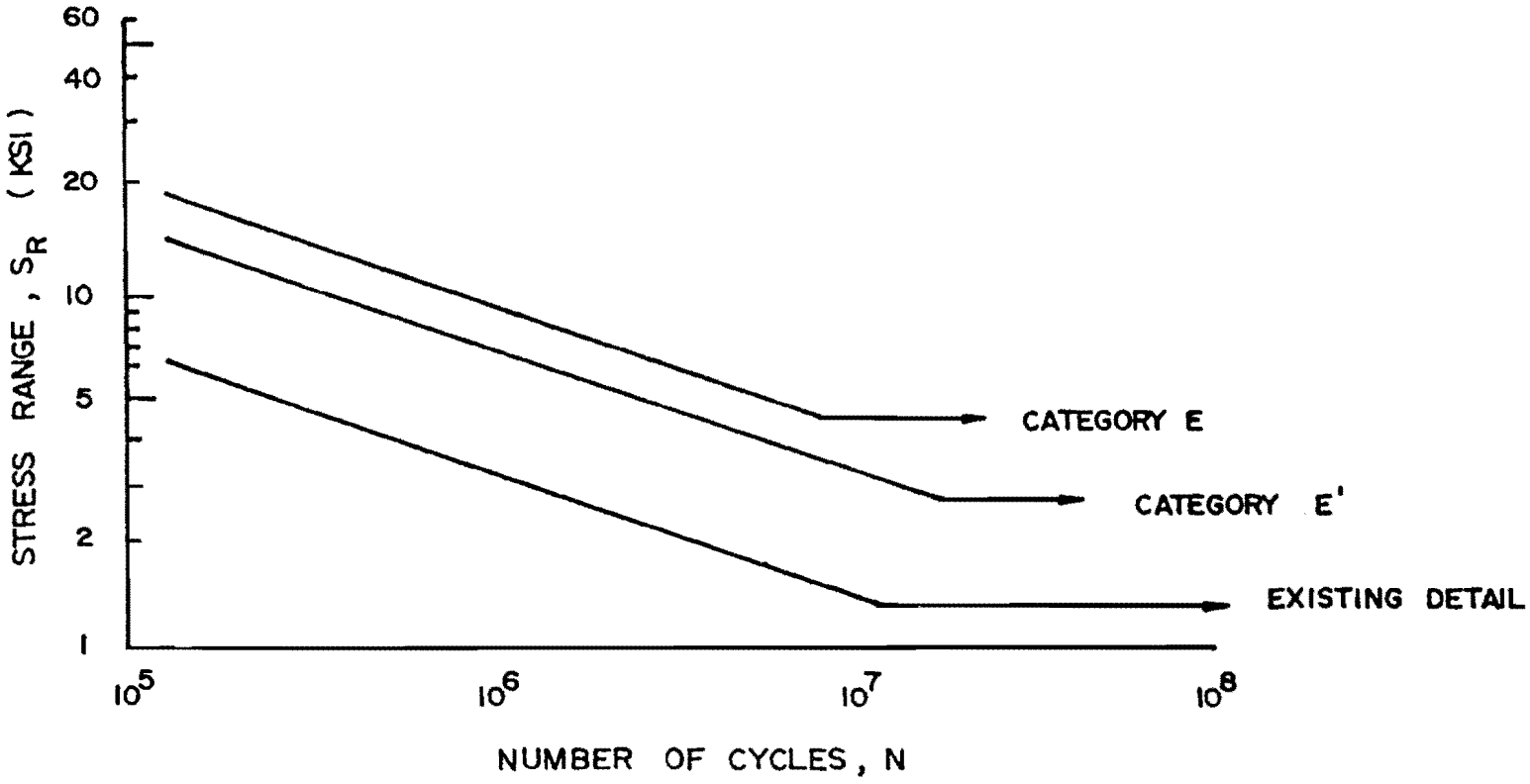

Fig. 1.4 Comparison of S_R-N relationship for the longitudinal-transverse stiffener detail

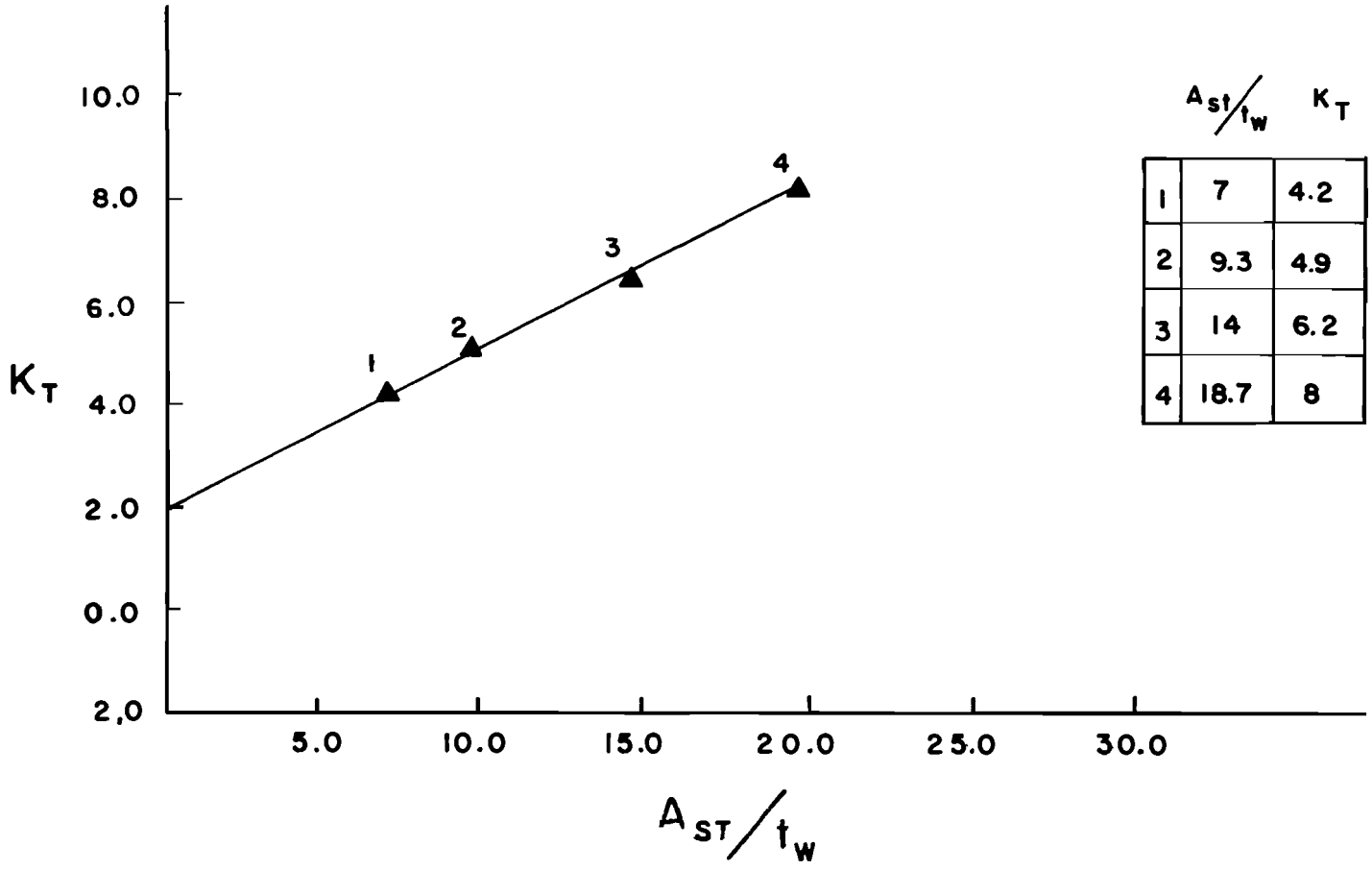

	A_{st}/t_w	K_T
1	7	4.2
2	9.3	4.9
3	14	6.2
4	18.7	8

Fig. 1.5 Effect of increasing the ratio of stiffener area to web thickness on stress concentration at the weld toe

length were varied. The specimen design will be discussed in Chapter 2. Chapters 3 and 4 present the testing procedure and results respectively. A discussion of the fatigue test results are given in Chapter 5, with a project summary and suggested retrofit procedures given in Chapter 6 and Appendix B respectively.

CHAPTER 2

EXPERIMENTAL PROGRAM

2.1 Background

Initial recommendations for the test specimens and the program were given by Platten [6]. His proposed specimens, shown in Fig. 2.1, were used as the starting point for selection of the fatigue test specimens. Although it would be more costly to fabricate due to its larger size, a beam test specimen rather than a tension test specimen was selected for testing. The beam type specimen is easier to test and more closely modeled the actual conditions in the bridge girder.

2.2 Specimen Design

Due to laboratory constraints, the specimen was limited to between 1/4 and 1/3 of actual scale. The depth of the beam was consequently limited to between 18 and 27 inches. Standard rolled sections were chosen to decrease fabrication costs. A 15 foot length was also chosen to accommodate space limitations.

The loading pattern shown in Fig. 2.2 was chosen because it provides a constant moment (no shear) region over the center of the span where the weld detail is located and also provides a constant moment region over a sufficient length of beam to fully develop the longitudinal stiffener.

Initial designs used the lightest W27 and W24 shapes available. A typical longitudinal stiffener size was chosen using criteria presented in the next section. The stiffener was placed at a distance $d/5$ from the bottom flange in accordance with section 1.7.43E of the 1977 AASHTO Bridge Specification in order to calculate the approximate section properties of the stiffened section. These properties were then used to determine the moment required to produce various nominal bending stress ranges at the level of the stiffener. Using this information and the loading system shown in

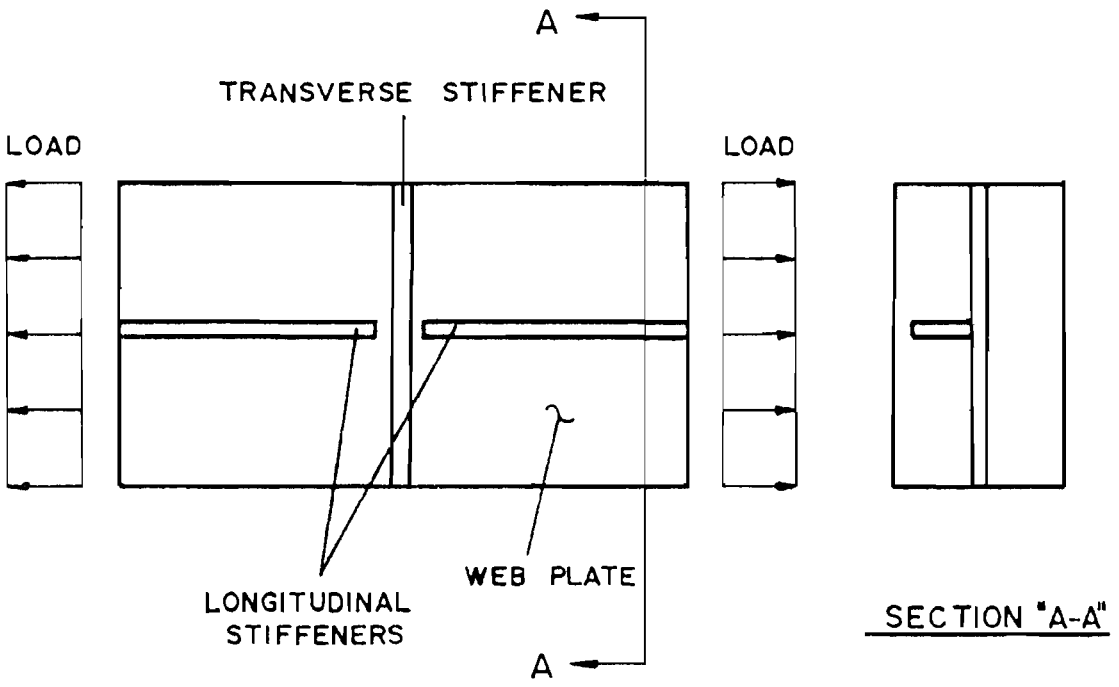

DIRECT TENSION TEST SPECIMEN

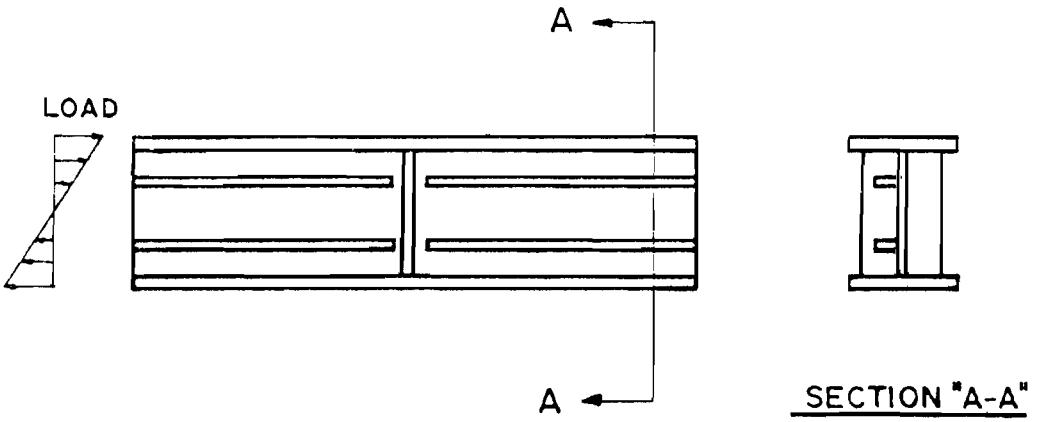

BEAM TEST SPECIMEN

Fig. 2.1 Two possible types of test specimens

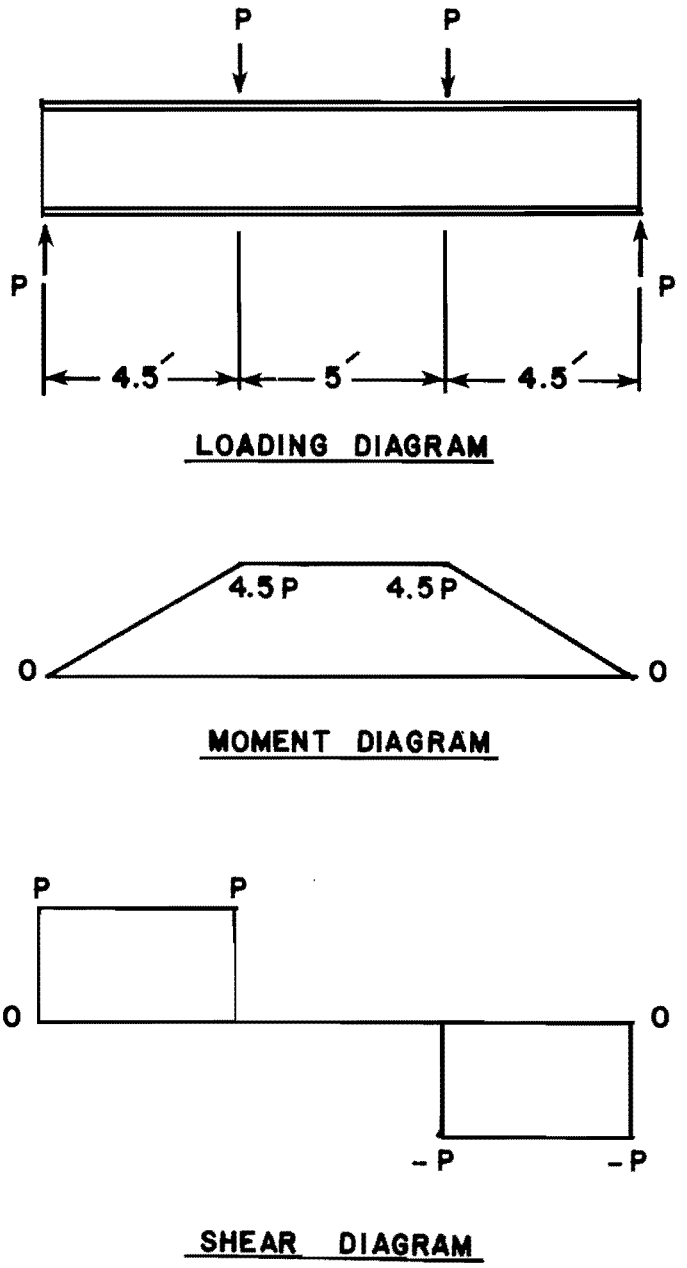

Fig. 2.2 Loading, moment, and shear diagrams of test specimen

Fig. 2.2, the required loads could be calculated and then matched to hydraulic jack capacities available in the laboratory. To produce the nominal stress ranges desired, up to 10^{ksi} at the stiffener intersection, a W21 x 44 beam was selected.

2.3 Longitudinal Stiffener Design

The results of Platten's finite element analysis were used to develop a relationship between the ratio of the area of the longitudinal stiffener, A_{st}, and the web thickness, t_w, and the stress concentration produced at the weld toe, K_t. The resulting relationship is shown in Fig. 1.5. The ratio on the actual bridge girder is:

$$A_{st}/t_w = \frac{b_s t_s}{t_w} = \frac{6" \times 7/16"}{3/8"} = 7 \qquad (2.1)$$

where b_s = width of the longitudinal stiffener and
t_s = thickness of the longitudinal stiffener

An A_{st}/t_w ratio of 7 was used on ten specimens to match the bridge girder. Four specimens were fabricated with $A_{st}/t_w = 5$ which were expected to show improved fatigue strength because of a reduced K_t as given in Fig. 1.5. A stiffener size of 4-1/2" x 3/8" was chosen for the ratio of 5; a 4-7/8" x 1/2" plate was chosen for the ratio of 7. These stiffener sizes satisfied the slenderness ratio requirements in AASHTO, Section 1.7.43E.

The longitudinal stiffener was placed at a 3" clear distance from the adjacent flange instead of the normal distance of one fifth of the beam depth or 3.7" clear distance. The 3" distance still permitted welding of both sides of the stiffener and also reduced the load required to produce the desired stress level at the stiffener.

2.4 Transverse Stiffener Design

The thickness of the transverse stiffener was the same as that on the existing detail with height and width adjustments to fit the test specimen. This was done to minimize scaling effects that would occur at the longitudinal stiffener intersection and would also allow the stiffener to meet the requirements of AASHTO, Section

1.7.43F1. A transverse stiffener 5-1/2" x 7/8" x 1'-7" was selected for all the specimens fabricated.

A 1/4" fillet weld for the longitudinal stiffener and a 5/16" fillet weld for the transverse stiffener were used to match the welds on the bridge girder.

2.5 Gap Size

The size of the gap between the end of the longitudinal stiffener and the transverse stiffener was shown by Platten to be an important variable. Increasing the gap size decreases K_t. Two gap sizes were selected for testing. First, the existing gap size of 1/2" was reproduced on the test specimens with the A_{st}/t_w ratio of 5 and 7. This would reproduce the existing detail conditions and would produce comparative data with only one variable, A_{st}, changing that could be checked against the finite element results. Second, specimens with an A_{st}/t_w ratio of 7 were fabricated with a clear gap width prior to welding of 2". This would produce data needed to verify the finite element analysis results on stress concentration at the weld toe relative to stiffener gap size. These three specimens are considered retrofit specimens and are discussed in Section 2.7.

2.6 Final Specimen Design

Figures 2.3, 2.4, 2.5 show the three different beam specimens used in the test program. Figure 2.3 shows the test specimen with an A_{st}/t_w of 5 and a gap size of 1/2". Figure 2.4 shows the details of the specimen with an A_{st}/t_w ratio of 7 and a gap size of 1/2". Figure 2.5 shows the details of the specimen A_{st}/t_w ratio of 7 and a gap size of 2".

2.7 Retrofit

Two basic methods of retrofit were considered to increase the fatigue life of the stiffener intersection. First, increase the gap between the stiffeners and second, make the longitudinal stiffener continuous. Both were suggested by Platten [6] but he only studied in depth the effect of gap distance between the transverse and the

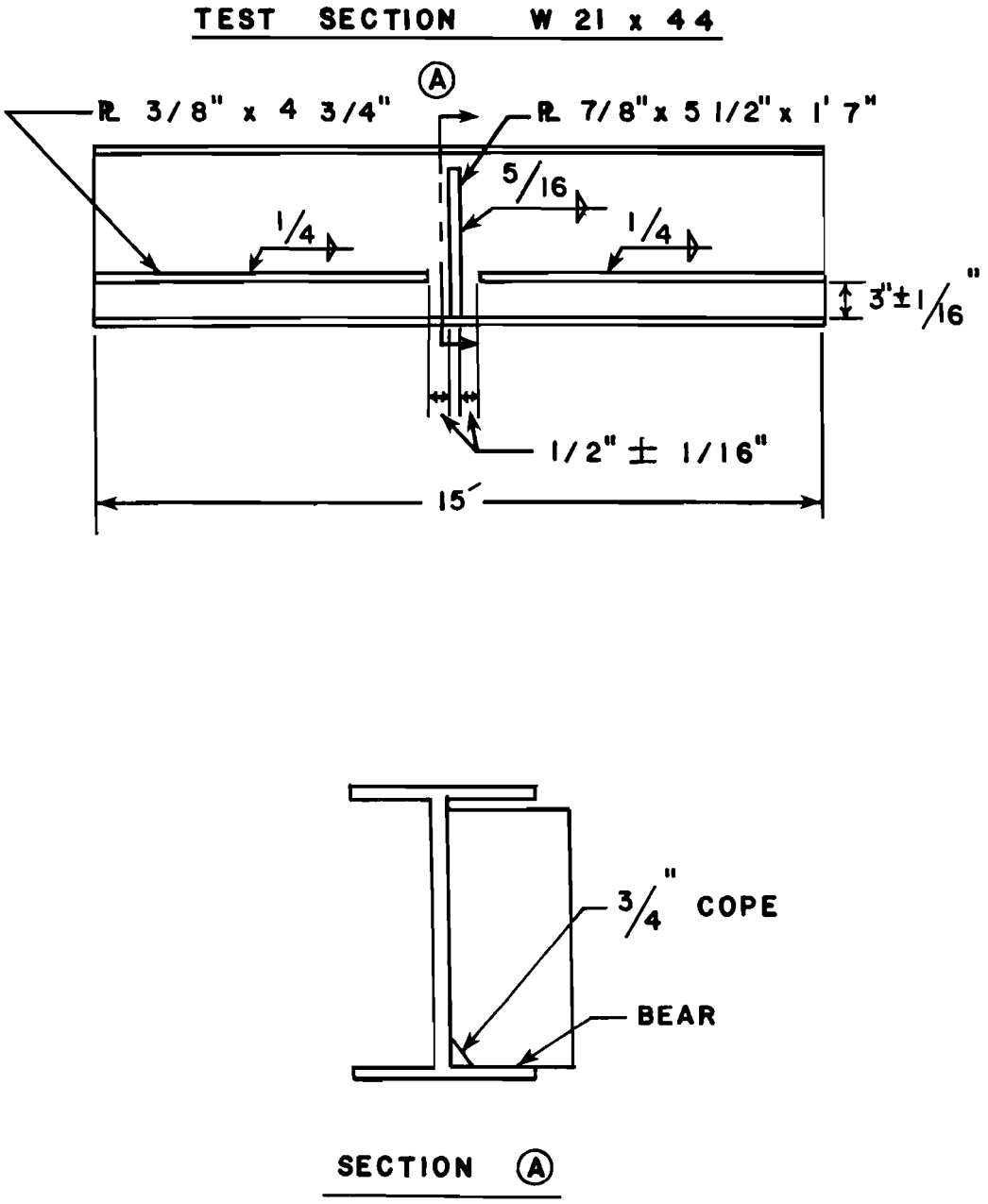

Fig. 2.3 Test specimen with A_{st}/t_w ratio of 5 and a 1/2" stiffener intersection gap

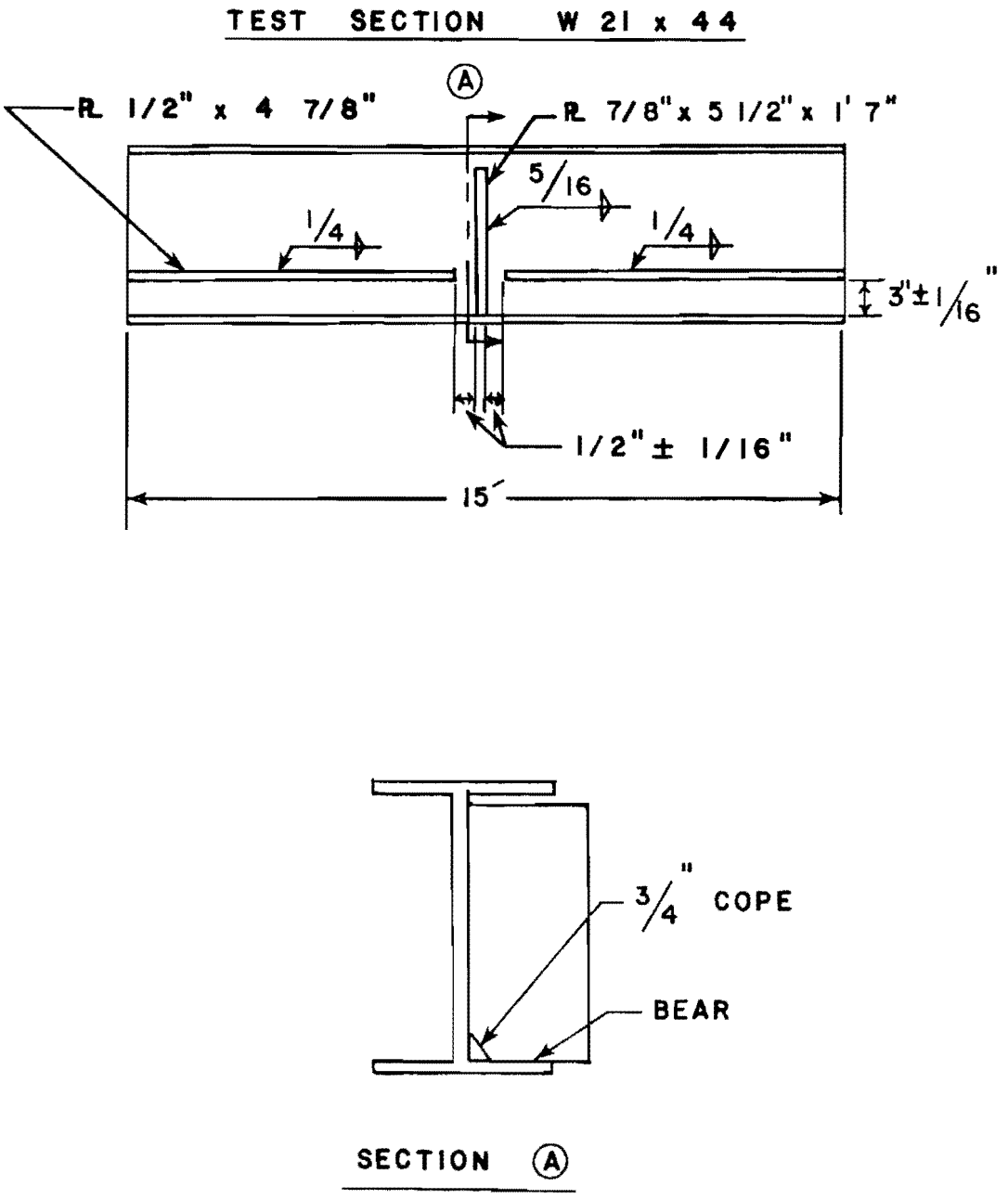

Fig. 2.4 Test specimen with A_{st}/t_w ratio of 7 and a 1/2" stiffener intersection gap

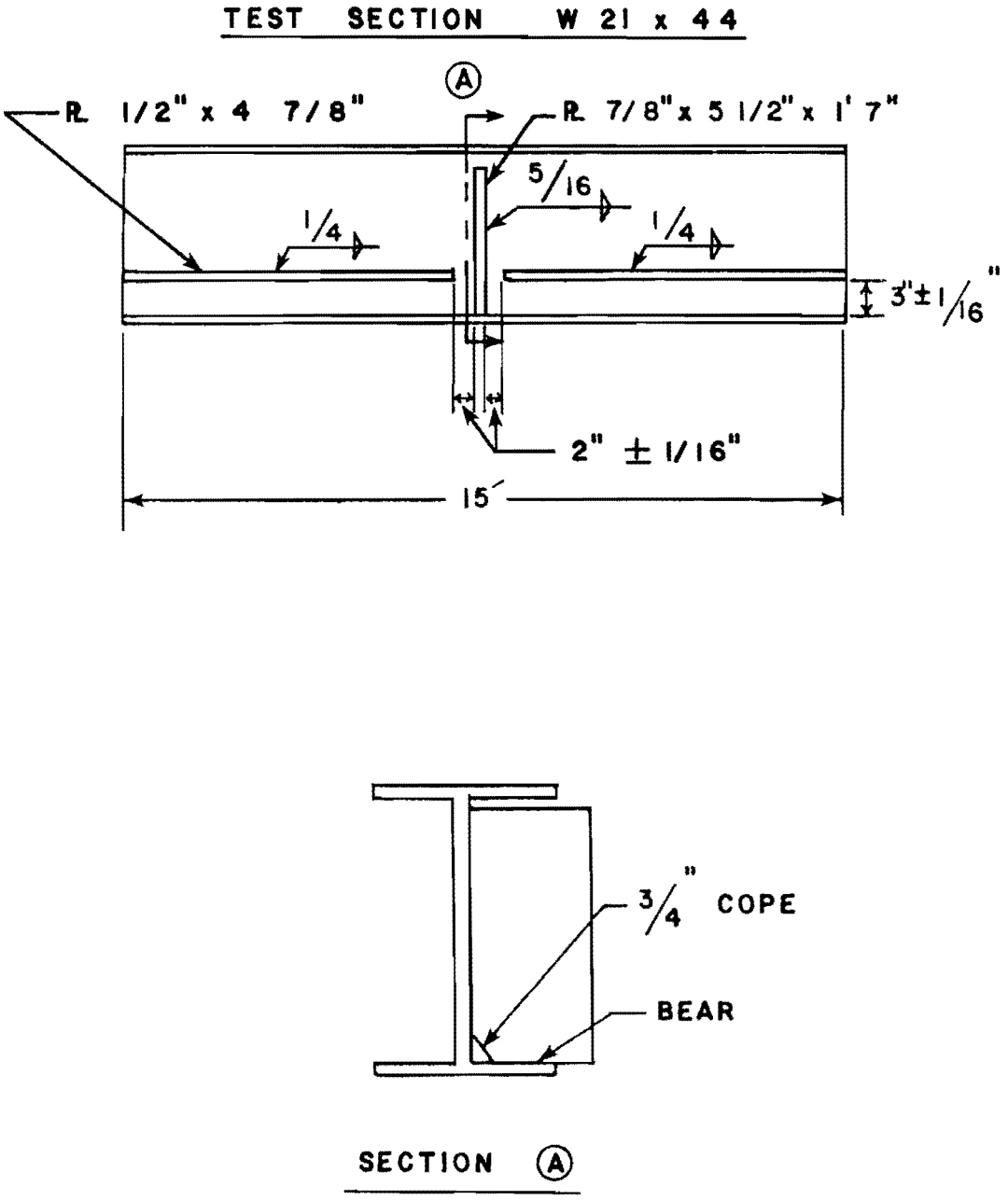

Fig. 2.5 Test specimen with A_{st}/t_w ratio of 7 and a 2" stiffener intersection gap

longitudinal stiffeners. Platten found that by increasing the gap from 1/2" to 2", the stress concentration factor at the weld toe was reduced 38%. By decreasing the stress concentration, an increase in the fatigue life was achieved. This prompted the design and fabrication of the three test specimens with the 2" gap which would be used to determine the validity of Platten's work. The second retrofit method attempts to make the longitudinal stiffener continuous by welding plates to both the transverse stiffener and the longitudinal stiffener as shown in Fig. 2.6. This effectively changes the longitudinal stiffener weld from a Category E to a Category C fatigue detail.

Four different welded plate retrofit specimens were tested. Three specimens had the same details. Two were run at different stress ranges, while the third was a repeat of one but the plates were welded on after a significant number of load cycles were applied to the specimen. The results from this specimen will indicate if possible damage prior to retrofit significantly alters the effectiveness of the retrofit detail. The fourth retrofit specimen, shown in Fig. 2.7 simulates the condition where a longitudinal stiffener is present on only one side of the transverse stiffener.

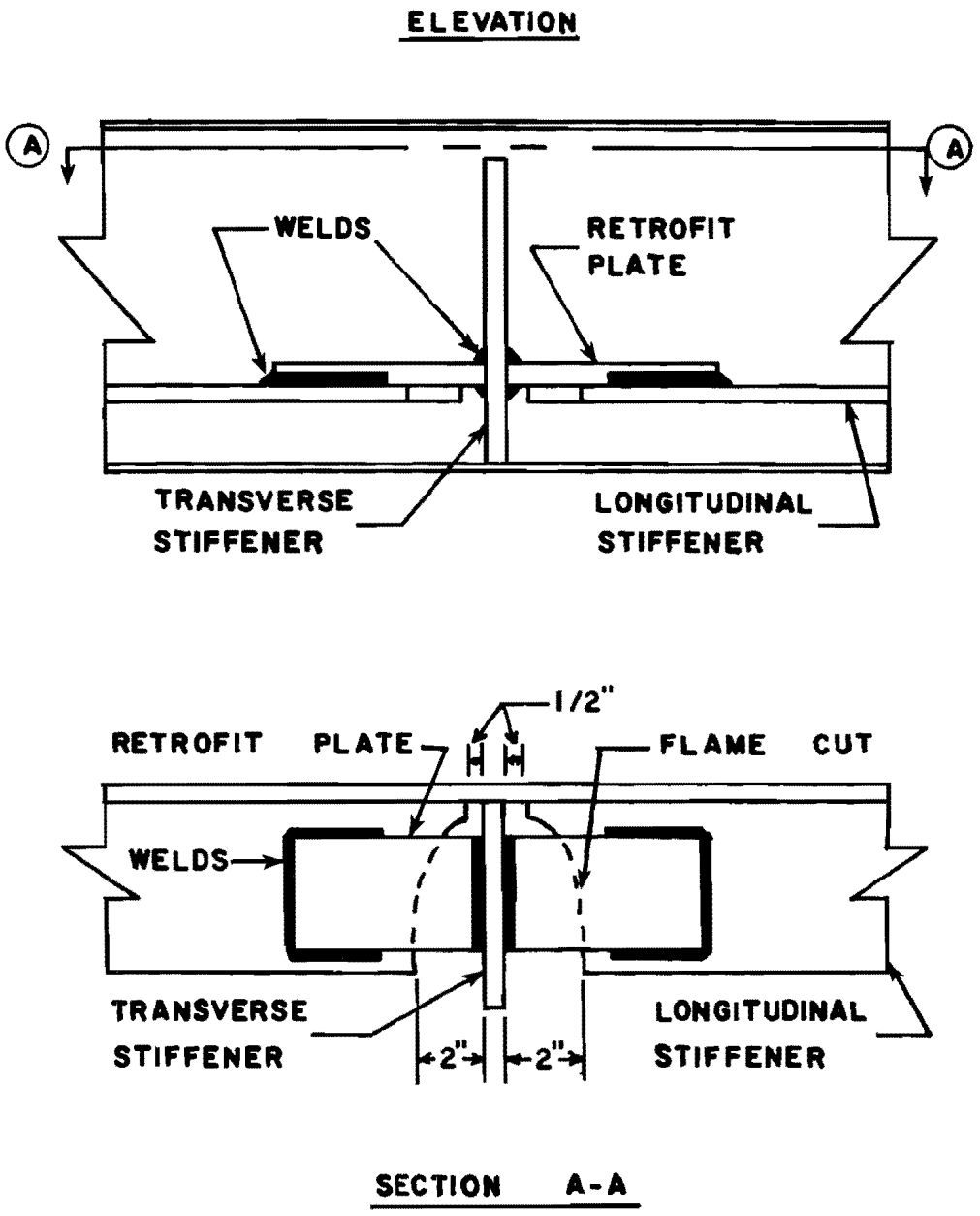

Fig. 2.6 Retrofit method

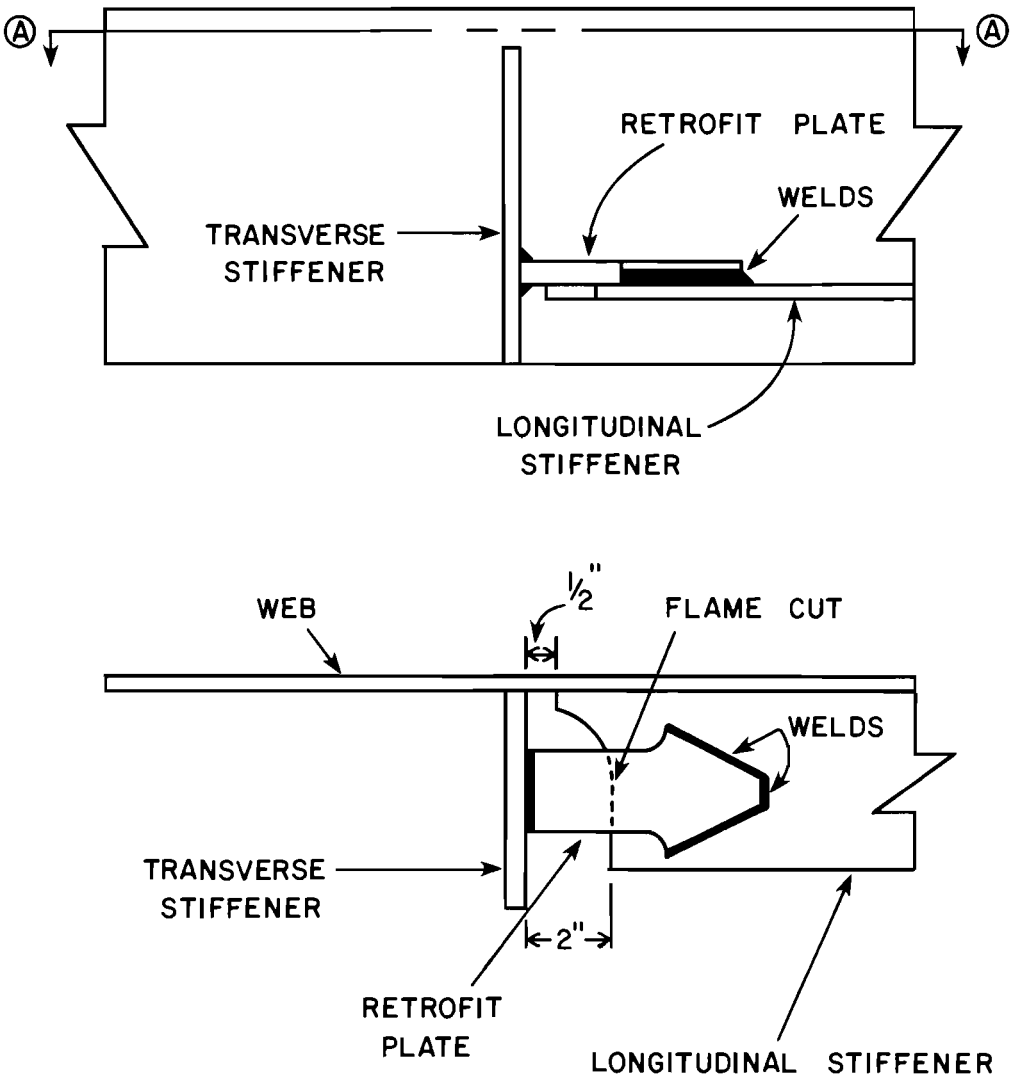

Section A-A

Fig. 2.7 One-sided retrofit specimen

CHAPTER 3

EXPERIMENTAL METHODS

3.1 Loading Setup

The test frame is shown in Figs. 3.1 and 3.2 The hydraulic testing ram supplying the load was supported by two 24" deep beams which were in turn supported by 12" deep columns at either end. The ram load was measured by a load cell which was attached to a spreader beam. The W10 x 88 spreader beam was used to transfer the load from the hydraulic ram to two load points five feet apart on the test specimen. A set of rollers mounted on the test specimen connected the spreader beam to the specimen. Rocker assemblies supported by pedestals which were post tensioned to a concrete floor slab supplied the simple end conditions for the test girder. In order to ensure that a minimal amount of out of plane bending was occurring, braces on the top and bottom flange of the test specimen were used.

The hydraulic ram shown in Fig. 3.3 has a dynamic capacity of 120,000 pounds. The hydraulic ram was connected to a Riehle-Los Universal Simple Acting Pulsator Type Fatigue Testing Machine. The schematic diagram is shown in Fig. 3.4.

Dynamic operation is developed by means of a piston assembly, shown in Fig. 3.4, mounted within the pulsator. The difference between the upper and lower load is proportional to the displacement of this piston which is controlled from the pulsator console. The loads are measured by two pressure gages, seen in Figs. 3.5 and 3.6, which internally monitor applied pressures through a series of rotary valves. These allow the fluctuating dynamic pressures to be read as a maximum and a minimum applied pressure.

The pulsator is powered by a variable speed drive connected to the crankshaft. The speed of the drive motor, and in turn, the frequency of the load oscillation is controlled by a potentiometer control at the console.

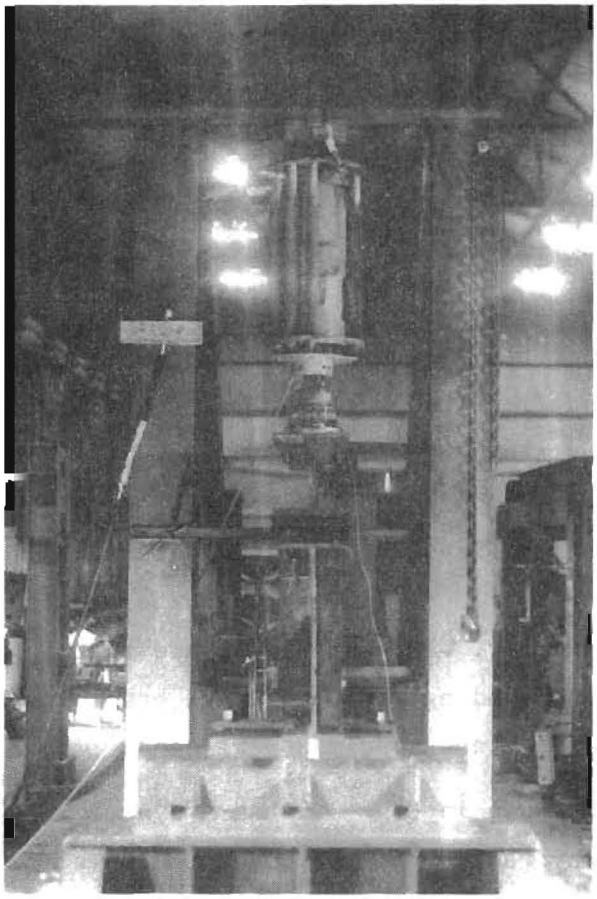

Fig. 3.1 End view of test frame

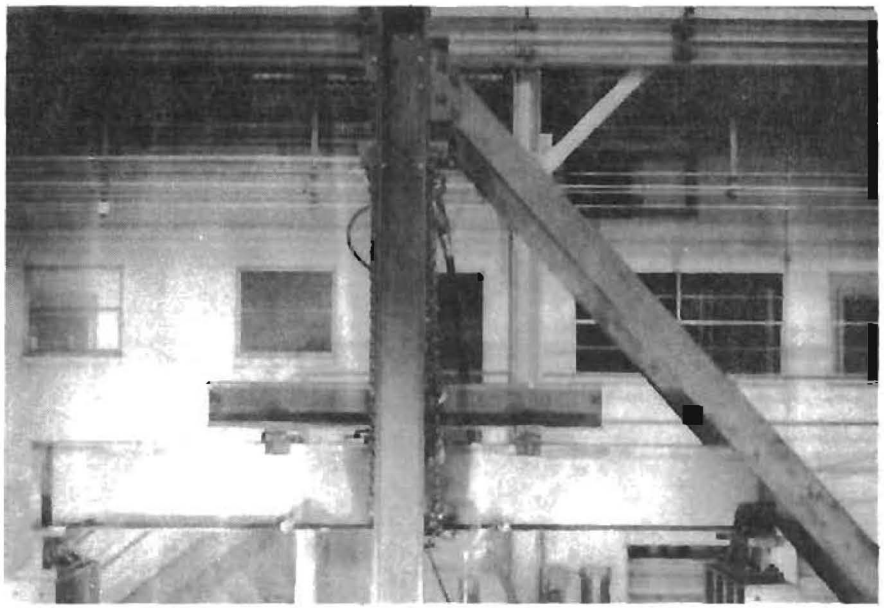

Fig. 3.2 Side view of test frame

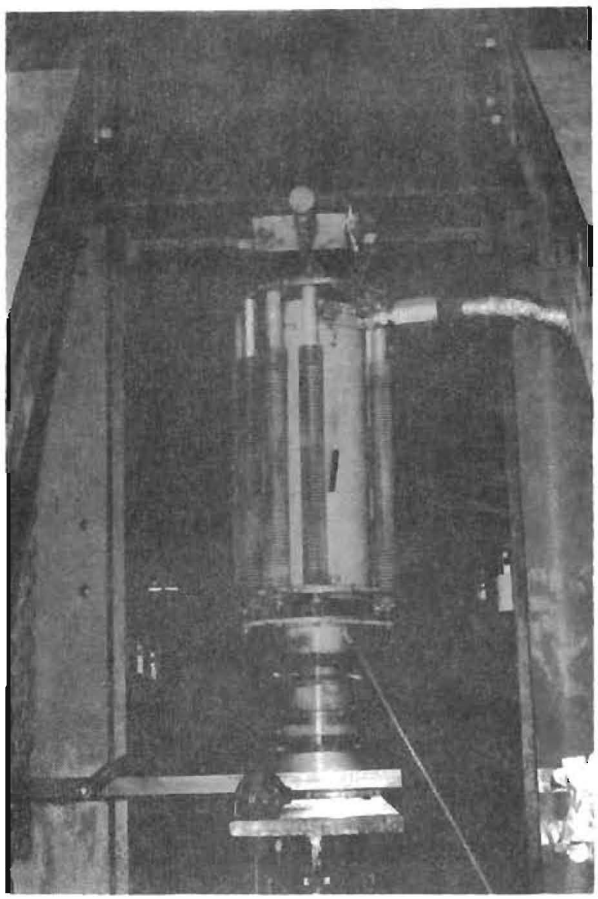

Fig. 3.3 Hydraulic test ram

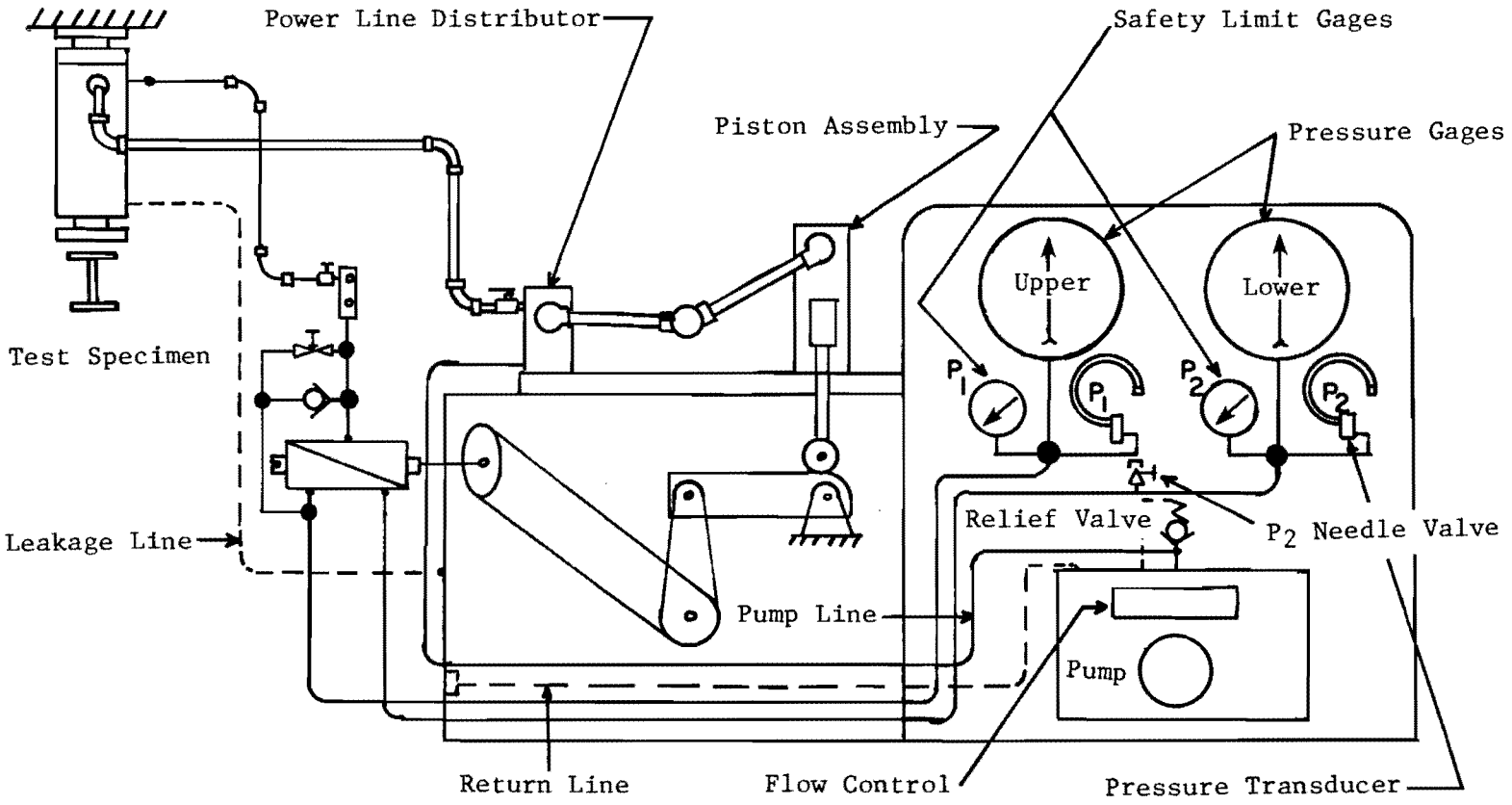

Fig. 3.4 Schematic diagram for the self-contained pulsator Riehle-Los Fatigue Testing Machine

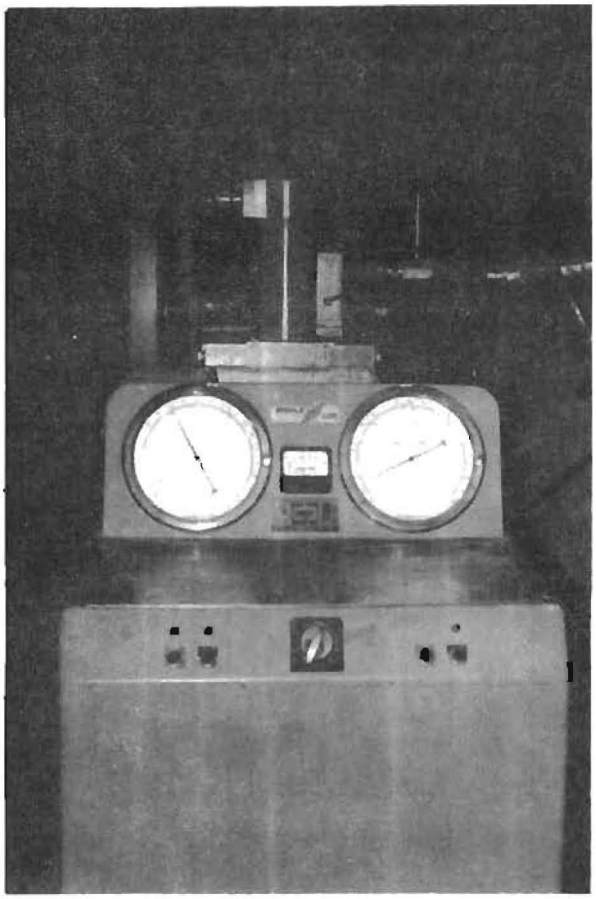

Fig. 3.5 Fatigue pulsator showing load pressure gages and front control panel

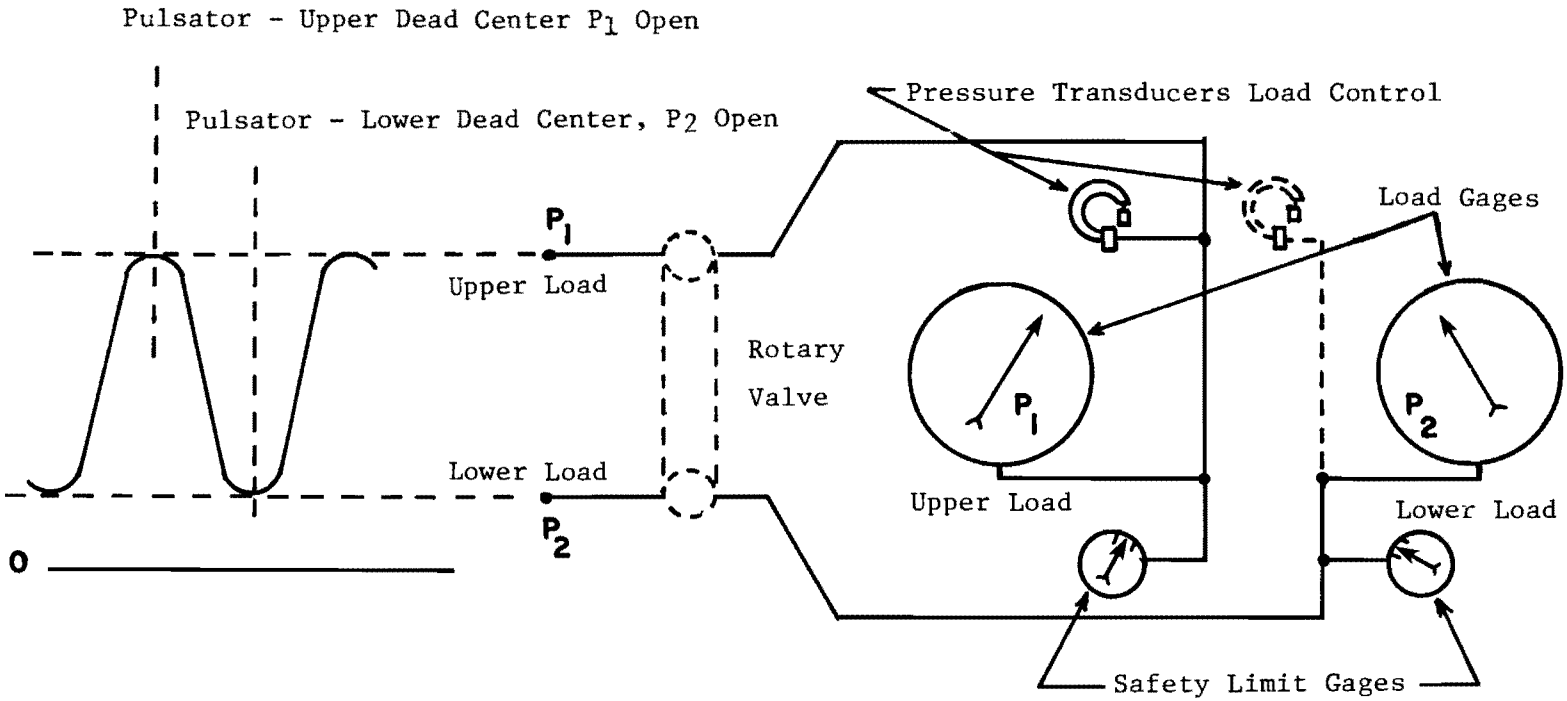

NOTE: P_2 load control optional, but required when arranged for program control

Fig. 3.6 Load indicating schematic diagram, single acting Riehle-Los Fatigue Testing Machine

3.2 Strain Gages

Three types of 120 ohm strain gages were used during the testing procedure. Foil gages with a .375 inch gage length and paper backed gages with a .64 inch gage length were used on all specimens except on the web of the retrofit specimens. There was no significant difference between the results obtained by the two different strain gages. In the retrofit testing phase, a foil gage with a gage length of .125 inches was used in the 2" gap specimen between the transverse and longitudinal stiffeners in order to determine the web strain in this region.

3.2.1 Specimen Strain Gaging

There were two basic strain gage patterns used during the testing program. Both of these patterns used the first two types of gages mentioned earlier - .375 inch foil gages and the .64 inch paper gages. The gage layout used for all fatigue tests is shown in Fig. 3.7. The eight flange gages would reveal if biaxial bending was occurring, if the loads were applied eccentrically or if there was an error in the applied load. The data was measured in a static loading performed prior to each fatigue test.

To determine cross sectional behavior, selected beams were more extensively gaged. The cross section was gaged with 40 gages (Fig. 3.8) in one test and 51 gages (Fig. 3.8 and 3.9) for two others. The extent of biaxial bending, the location of the neutral axis, load carrying characteristics of the longitudinal stiffener, and the nominal stresses in the web at the level of the longitudinal stiffener were determined.

3.2.2 Strain Gage Installation

The gage location was marked and then ground smooth using a high speed hand grinder. The surface was cleaned with acetone, etched with a mild acid and then neutralized by a basic solution. The site was then wiped clean and dry. A special adhesive was

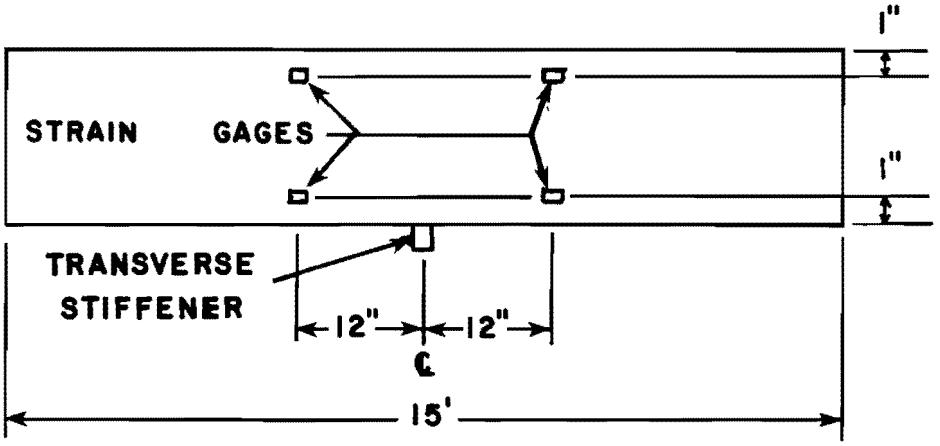

Fig. 3.7 Strain gage set up, fatigue test

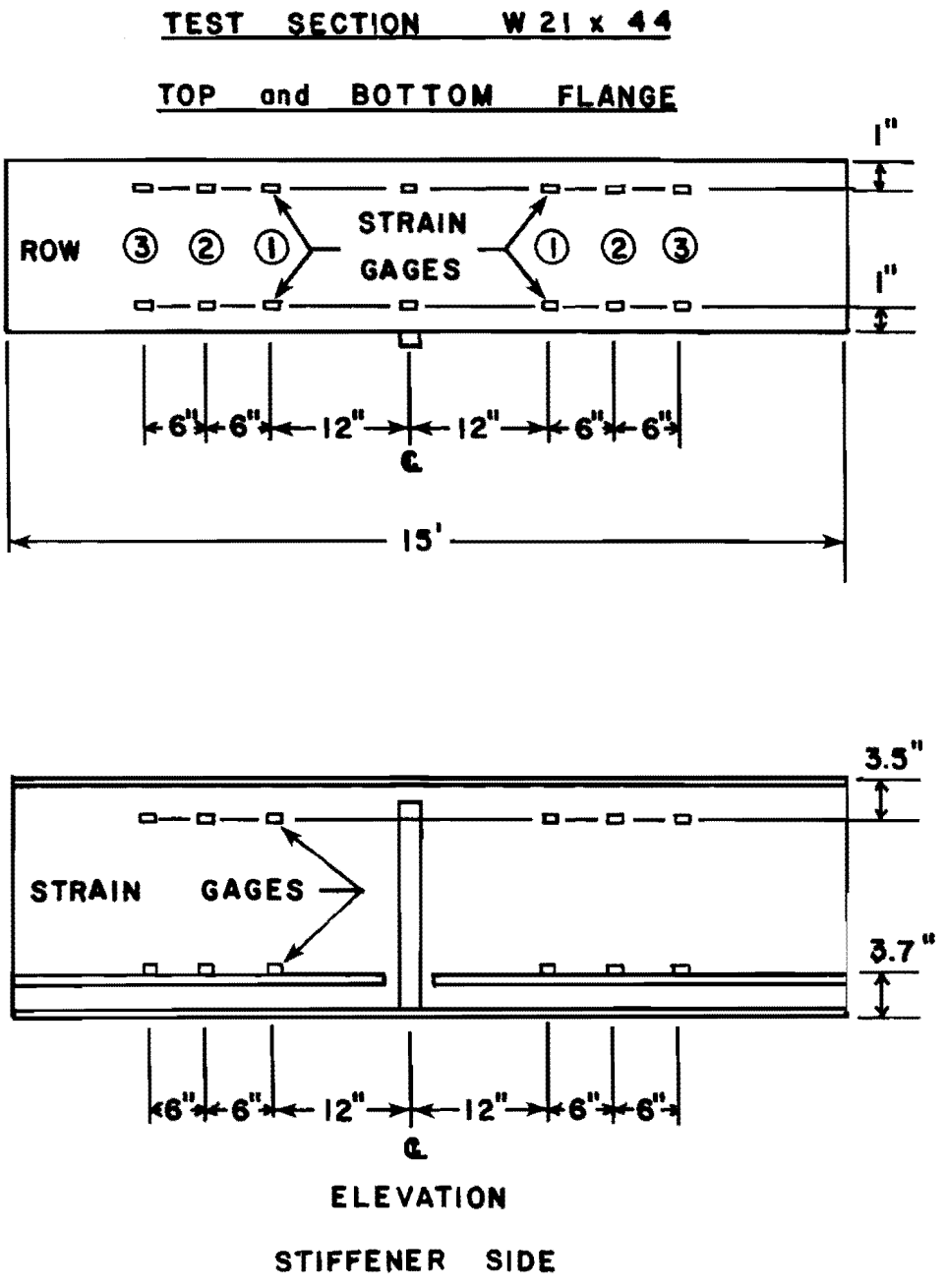

Fig. 3.8 Typical strain gaging, static test

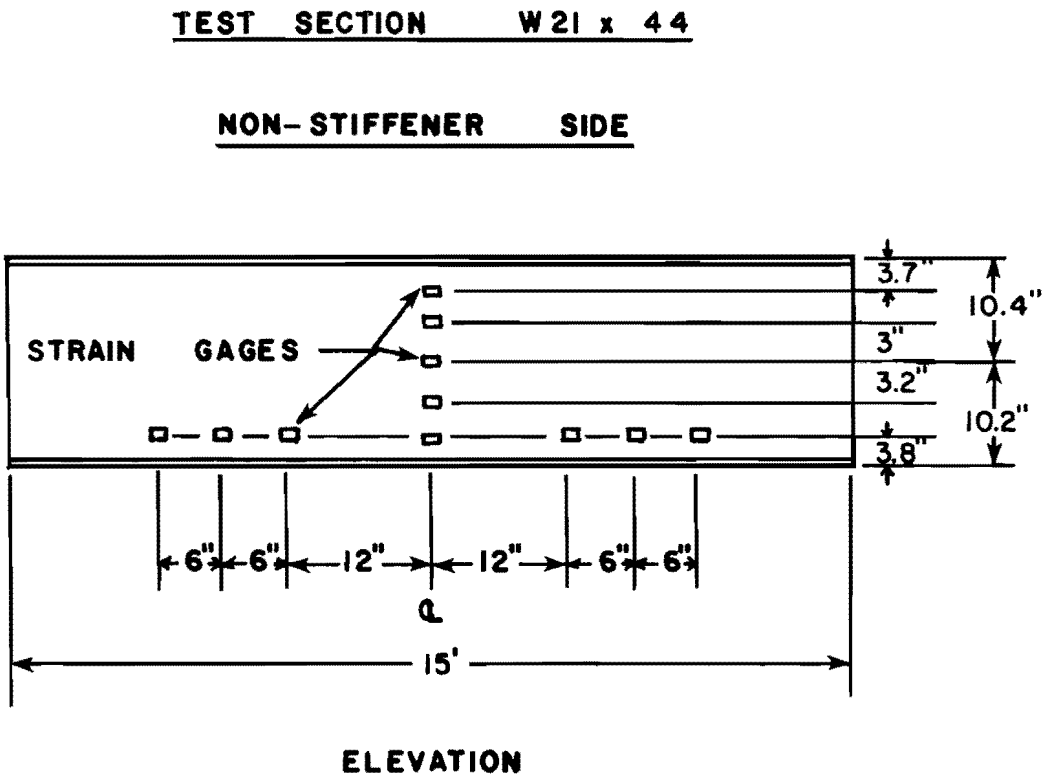

Fig. 3.9 Additional strain gages used for a static test with 51 gages

applied to the beam and a catalyst applied to the back of the strain gage. The strain gage was placed on the beam and excess glue was then squeezed from under it. A barrier material was then placed on top of the gage for protection.

Wires were then soldered to the leads of the strain gage and secured to the test specimen by an adhesive backed rubber pad. The wires were then connected to a portable strain indicator. A separate strain indicator was used to monitor loads on the load cell.

3.3 Test Procedure

Initially, section characteristics (height, width, thickness) of the specimen were measured and bending axis section properties with and without the longitudinal stiffener calculated. Using the formula, My/I_x, loads were computed to provide a nominal stress at the level of the stiffener of 2^{ksi}, 5^{ksi}, 10^{ksi}, and 12^{ksi}.

Static tests were performed at these stress levels before every fatigue test. At each stress level, the applied load was monitored using the load cell as well as the load gage on the pulsator. This ensured checks on the applied loadings. The fatigue tests were performed at specific stress ranges, S_R. The stress range was to be the nominal stress range at the level of the stiffener with a minimum stress in all specimens of 3^{ksi}. The minimum and maximum loads were set on the pulsator to produce the desired stress range. The minimum load was set on the pulsator and the corresponding vertical deflection of the beam at gage 1 in Fig. 3.10 was recorded. The maximum load was then set and the corresponding deflection read from gage 2. Both load levels were also monitored with the load cell. The deflections recorded corresponded to the loading required to produce the desired S_R.

The next step was to set the two deflection gages at their corresponding deflections recorded above (i.e., gage1, minimum load; gage 2, maximum load). The pulsator was then adjusted to produce dynamic deflections which matched the static values. This method of setting the dynamic loads compensated for any dynamic loading effects.

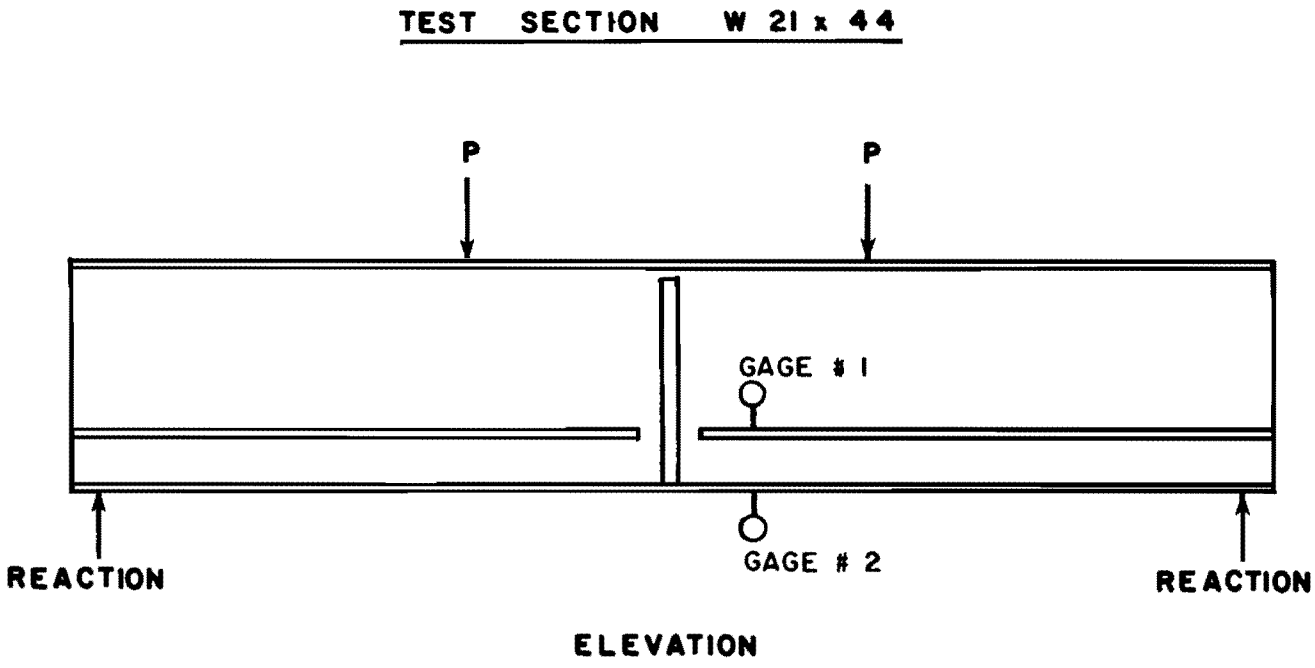

Fig. 3.10 Location of mechanical deflection gages to monitor deflections from applied loads

The dynamic loads measured on the pulsator were within 3% of the static values.

The load range was kept constant during each test and periodically the cyclic action was stopped for examination of the specimen. Specimen loading was continued until a crack penetrated through the web thickness and extended a few inches into the web depth.

CHAPTER 4

TEST RESULTS

4.1 Load Calibration

Fig. 4.1 shows the results of the load cell calibration which indicates the error between the applied load as indicated by a calibrated load cell and the applied load as indicated by the pulsator-ram assembly to be approximately 2%. This error was compensated for during testing.

The load cell was used to monitor loads applied by the pulsator during testing and showed the applied loads to fall within ±3% of the applied load indicated by the pulsator gages.

4.2 Specimen Chemistry and Mechanical Properties

Test specimens were ordered in two separate groups. The four specimens with a nominal A_{st}/t_w ratio of 5 were ordered first with the remaining ten ordered several months later.

To better compare the specimens and fatigue test results, a chemical analysis and static tension test was performed on two specimens from the rolled beams used for each group. The results are shown in Table 4.1. Although there are slight differences, they are minor and were not considered to be large enough to cause a significant difference between results from the two sets of test specimens. Both sets meet the requirements of ASTM A36 steel.

4.3 Test Specimen Cross Section

The cross sections chosen for testing, shown in Fig. 4.2, presented some interesting problems concerning behavior under load and modeling of the actual bridge girders. The major concern was the effect of the longitudinal stiffener on the behavior under load.

A typical cross section for the actual bridge girder is shown in Fig. 4.3. The size of the longitudinal stiffener relative to the

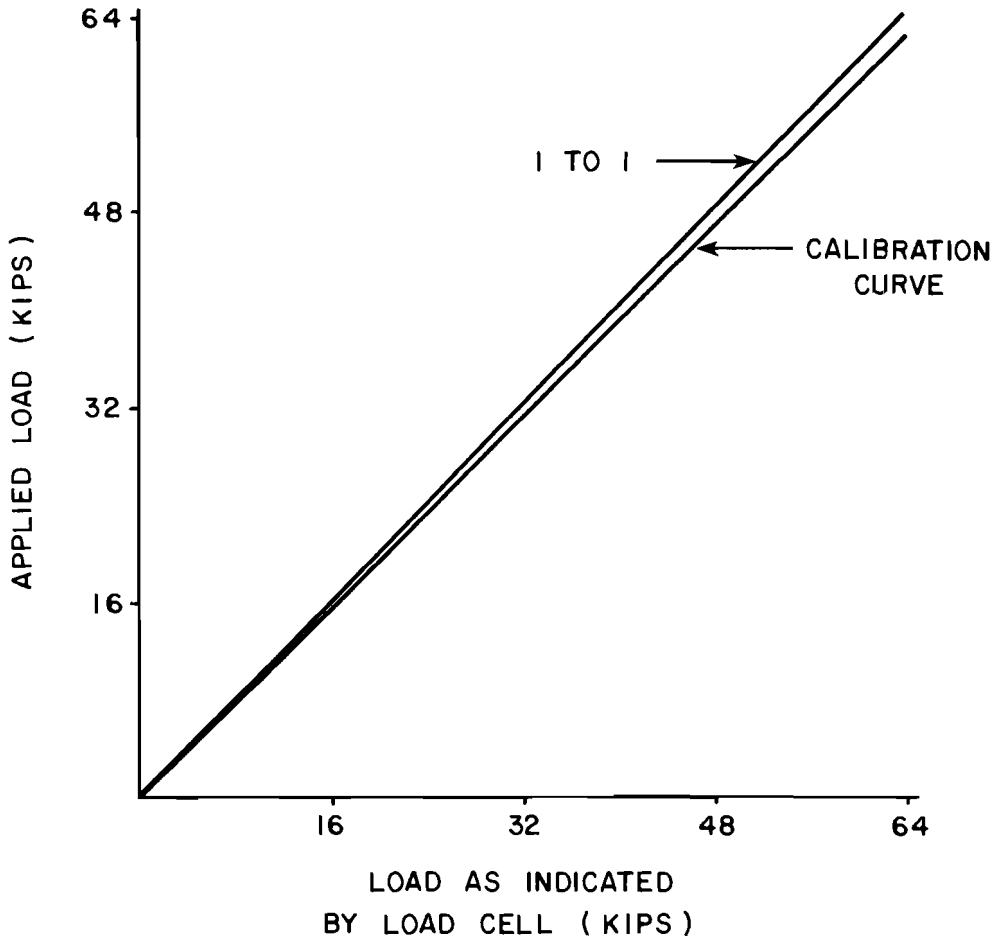

Fig. 4.1 Load calibration curve

Table 4.1 Chemical Content of Test Specimens

GROUP	C (%)	Mn(%)	P(%)	S(%)	YIELD STRENGTH (ksi)	ULTIMATE STRENGTH (k)	% ELONGATION
$A_{st}/t_w = 5$	.20	.60	.011	.025	40.4	65.24	31
	.22	.64	.003	.023	43.1	67.43	30
$A_{st}/t_w = 7$	.19	.82	.007	.022	48.6	69.02	27
	.19	.82	.007	.022	44.2	64.46	29

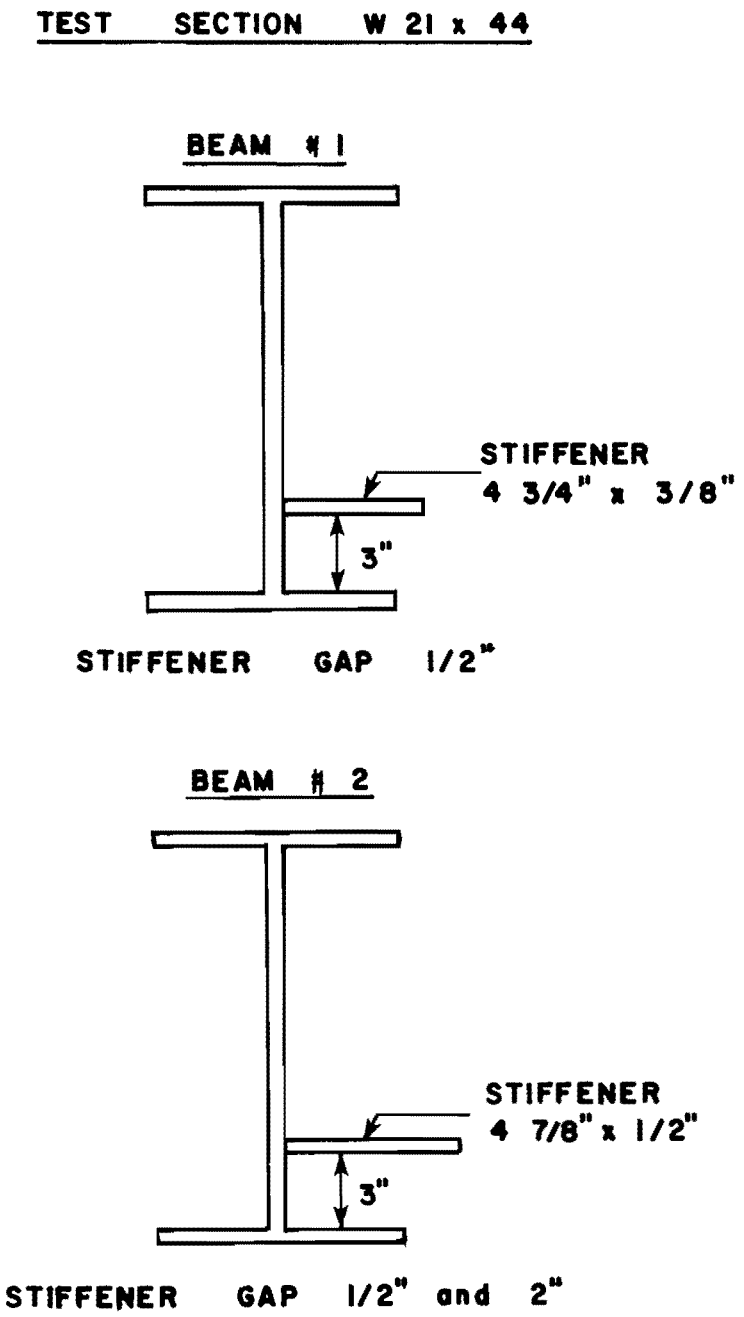

Fig. 4.2 Test specimen cross sections

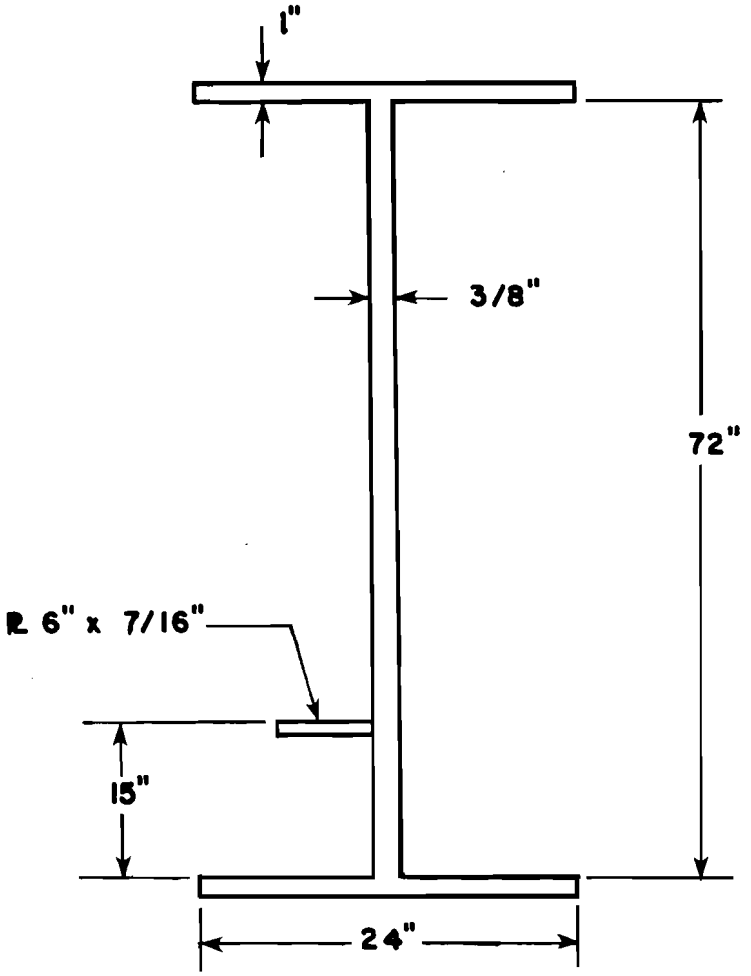

Fig. 4.3 Typical bridge girder cross section

overall cross section is small which means the stiffener has a small effect on the moment of inertia and the location of the neutral axis. Section properties and the effects of the stiffener on the section properties were studied in the early part of the test project by GUPTA [7]. He reported that the effects of the longitudinal stiffener on the section properties were small enough to be hidden by the range of his experimental reliability. From his data he also concluded that little weak axis bending was occuring in the actual bridge girder. This is not the case with the test specimens. Table 4.2 compares the changes that occur to the section properties of the two test specimens in Fig. 4.2 and those of the full size bridge girder, shown in Fig. 4.3, due to the addition of each sections' longitudinal stiffener.

The relative changes in the section properties due to the longitudinal stiffener is considerably larger in the test specimens, also the stiffener addition causes a rotation of the principal axes and a shift in the shear center from the centerline of the web. Fig. 4.4 shows the results of an analysis to determine the principal axes rotation and shear center location on a typical test beam.

The rotation of the principal axes by 1.76° changes the principal moments of inertia by about one-tenth of one percent. This does not cause any significant bending problems. The shift in the shear center of .51 inches will cause torsional moments in the section when it is loaded in the plane of the web. Three braces were used on the test specimen to minimize effects of out of plane bending and torsion on the test cross section. Two braces on the top, six inches from the centerline of the beam, and one on the bottom, also six inches from the centerline of the beam, were used. One brace was also used on the spreader beam to provide overall stability to the test set-up.

4.4 Cross Section Behavior

Three static tests were performed on the test section in addition to the tests performed prior to dynamic testing. These

Table 4.2 Comparison of Section Property Changes due to Stiffener Addition to Bridge Girder and Test Specimens As Seen in Figures 4.1 and 4.2

SECTION	AREAS (in^2) A_f	A_w	A_{st}	$\frac{A_{st}}{A_t}$	$\bar{y}$, INCHES (FROM BOTTOM FLANGE) WITH STIFF	W/O STIFF		% of d	I_x (in^4) WITH STIFF	W/O STIFF	Δ	% of I_x W/O STIFF
BRIDGE GIRDER FIG. 4.3	48	27	2.625	3.3%	36.26	37	.74	1%	76,840	75,616	1224	1.6%
BEAM #1 DYNAMIC SPEC. 3 Fig. 4.2	5.77	6.76	1.77	12.4%	9.5	10.3	.8	3.9%	874	806	68	7.8%
BEAM #2 DYNAMIC SPEC. 4 FIG. 4.2	6.04	7.65	2.41	15%	9.3	10.3	1	4.9%	897	806	91	9.6%

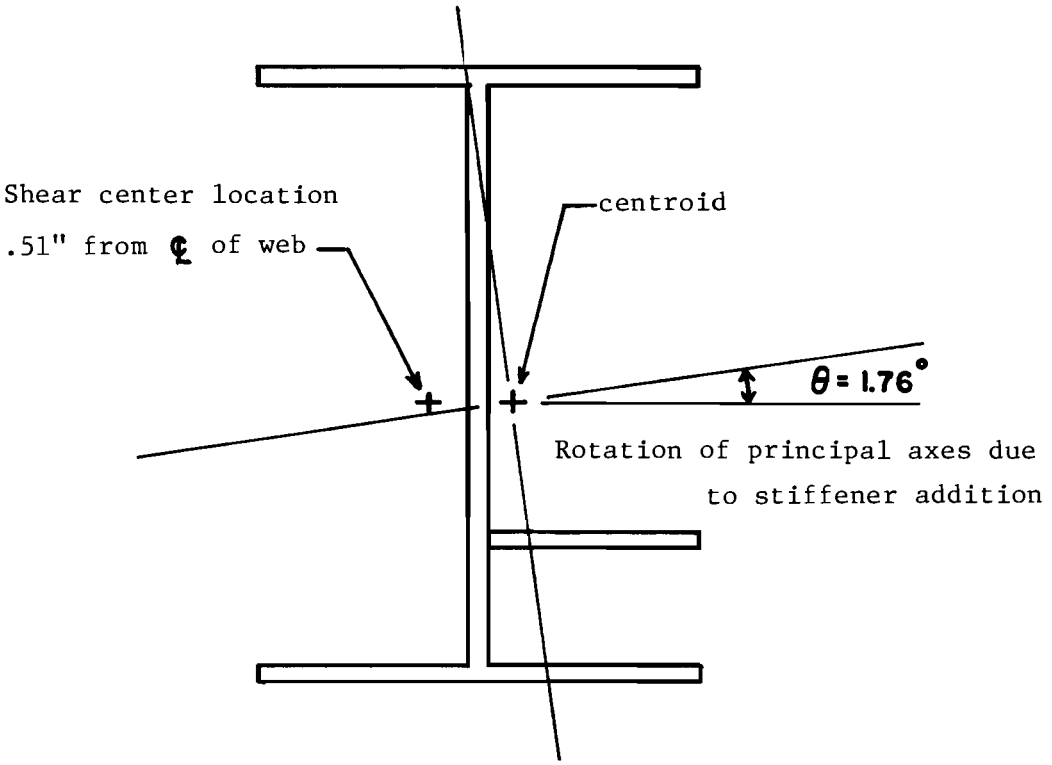

Fig. 4.4 Figure showing rotation of principal axes and location of shear center on a typical test section

tests were performed to determine whether the amount of out of plane bending or cross bending was excessive, the location of the neutral axis along the length of the beam, the distance needed for the longitudinal stiffener to become fully effective, and whether a cross section of beam at the stiffener intersection behaved as a stiffened or unstiffened section.

4.4.1 Static Test Procedure

In the elevation view in Fig. 4.5 the symbols (x) illustrate where the braces are located.

The first test was performed using the gage set-up shown in Fig. 3.8 and two braces, both on the compression flange. The second test used the gage set-up in Figs. 3.8 and 3.9 and two braces as above. The third test was the same as the second except an additional brace was placed on the tension flange. Only the results of the second and third tests will be discussed as the first and second were essentially duplicates.

For both tests, a series of four different load levels were monitored three separate times. For example, a load of 10 kips was applied, the strain gage readings taken, the load increased to 20 kips, the strain gage readings taken, etc. up until 40 kips had been applied. The load was then dropped to zero, all gages rezeroed and the entire sequence performed two more times.

The loads were calculated using elastic flexure theory with the moment of inertia of an unstiffened cross section to produce nominal stresses at the level of the stiffener of 2^{ksi}, 5^{ksi}, 8^{ksi} and 10^{ksi}. These calculated loads do not necessarily correspond to the loads used in the example above.

Fig. 4.5 depicts the basic physical action that occurs during bending. The beam is subjected to an inplane moment causing compression on the top fibers and tension on the bottom fibers. Looking only at the compression flange, if the beam deflects in a vertical plane, the compression on all the fibers an equidistance from the

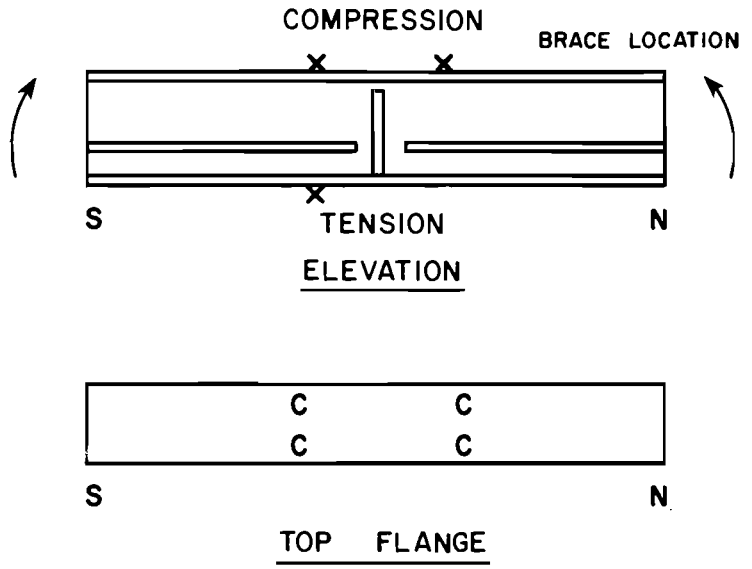

Fig. 4.5 Beam bending with no out of plane movement

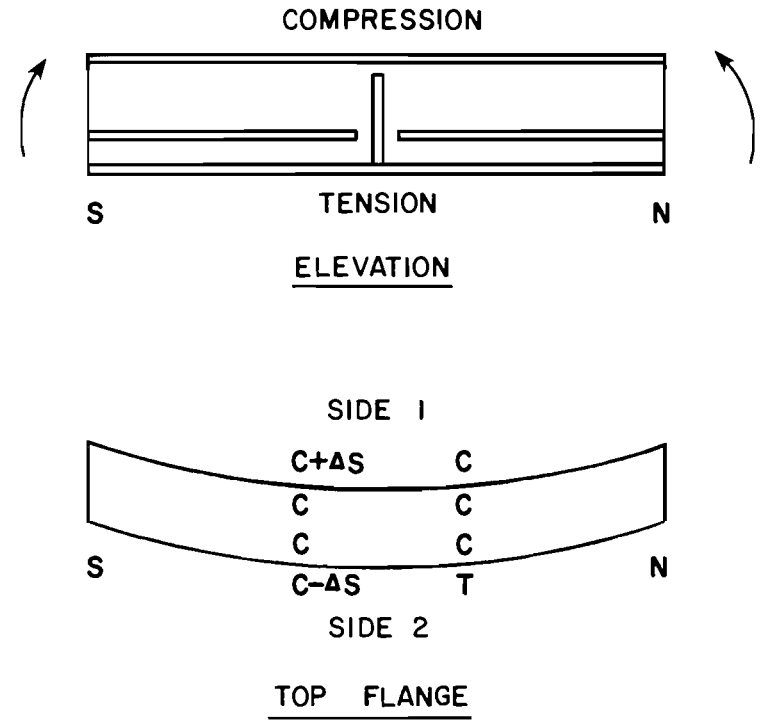

Fig. 4.6 Beam bending with out of plane movement

neutral axis will be the same. However, if the beam bends out of plane, as in Fig. 4.6, not only is there compression on the top fibers but there is also compressive and tensile stress, shown as ΔS, due to the out of plane bending. This causes higher compressive forces on one side of the top flange, shown as side 1 in Fig. 4.6, and lower compression forces on the opposite side, side 2. These differences can be measured using strain gages. In the test specimens, the tendency was to bend out of plane in the direction of the stiffener.

4.4.2 Out of Plane Bending Results

Fig. 4.7 is typical of the flange strain data results collected during the second static test and is used to illustrate the amount of out of plane bending. This figure shows points collected at a load level of 37.4 kips which corresponds to 8^{ksi} at the level of the stiffener. The points were normalized by dividing the stress calculated using elastic flexure theory and the properties of the stiffened section, σ_c , by the measured strains, σ_m . The strain gage readings were converted to a stress using a modulus of elasticity of $29{,}000^{ksi}$. Since each different load level was repeated three times, there were three points for each gage location at each load level. The average of this data is shown in Figs. 4.7 and 4.8.

Fig. 4.7A shows a relatively constant stress ratio indicating very little out of plane bending. Since the top flange had two braces on it this is a reasonable result.

The bottom flange readings, Fig. 4.7B, indicate a different behavior. The readings at the centerline indicate significant out of plane bending which decreases and changes sign away from the centerline of the section.

After comparing the compression and tension flange readings on this test, out of plane bending appeared to be a problem on the tension flange more than on the braced compression flange. This prompted the use of a brace on the tension flange in the third test.

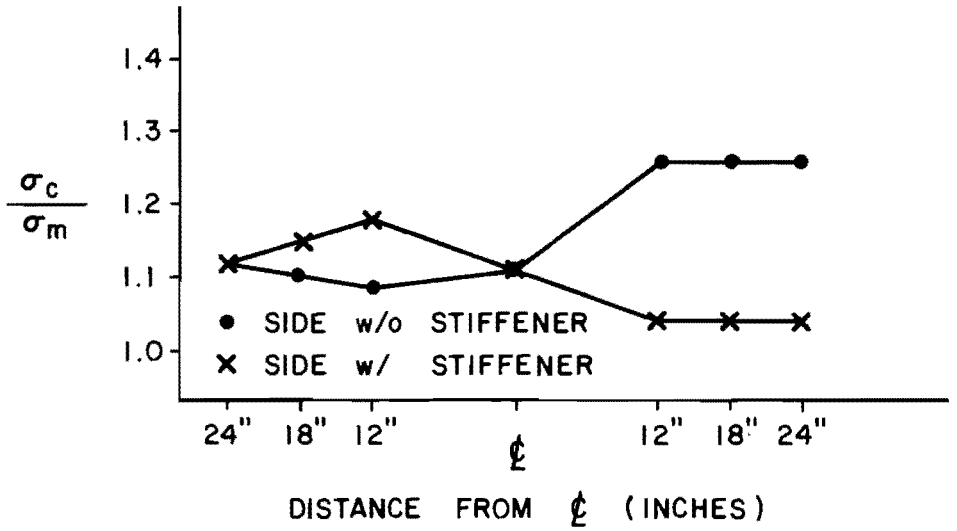

A) Top Flange

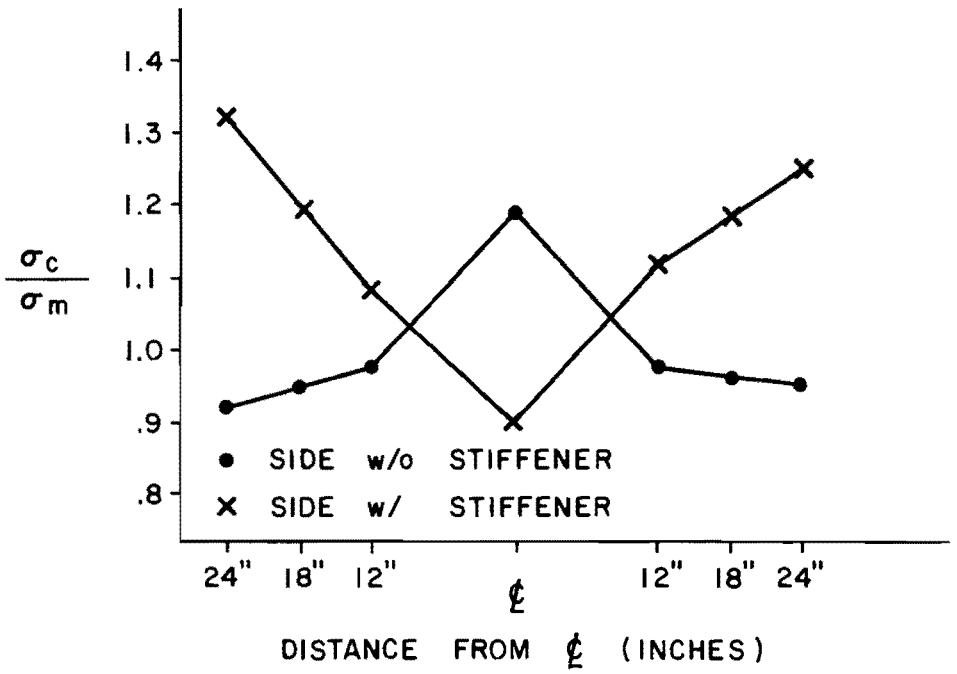

B) Bottom Flange

Fig. 4.7 Flange strain data for second static test P=37.4^k

Fig. 4.8 is typical of the results of the flange strain data collected during the third static test. General trends show the same results as the second test for the top flange, Fig. 4.8A. There is little out of plane bending. The bottom brace decreased the effects of out of plane bending on the tension flange (Fig. 4.8B) over the region 24 inches either side of the centerline. The only other significant change appears to be at the centerline where a sharp change in the stress level is seen. This is probably due to the change in the section due to the interruption of the longitudinal stiffener.

The results showed that, with the use of the tension flange brace, out of plane bending could be reduced enough in the region of the stiffener intersection that its effects would not influence the fatigue test results.

4.4.3 Neutral Axis Location and Stiffener Effectiveness

Stiffener effectiveness and neutral axis location are closely related. As the stiffener becomes effective it becomes part of the bending cross section. This causes a shift in neutral axis location and an increase in the stiffness, moment of inertia, due to the additional effective stiffener material.

There were two different experimental methods used for computing the location of the neutral axis; 1) using flange gages, 2) using web gages at the centerline of the span. With the flange gages, the neutral axis was calculated separately for each row of gages (see Fig. 3.8) to determine the shift in neutral axis location due to increased stiffener effectiveness. Compression and tension gages were averaged to get the upper and lower strain readings used to compute this location. Using the web gages at the centerline (see Fig. 3.9) only the neutral axis location at the centerline could be determined.

Flange gage results from the second test without the tension flange brace can be seen in Fig. 4.9. The neutral axis location moves slightly towards the bottom of the test specimen as you move

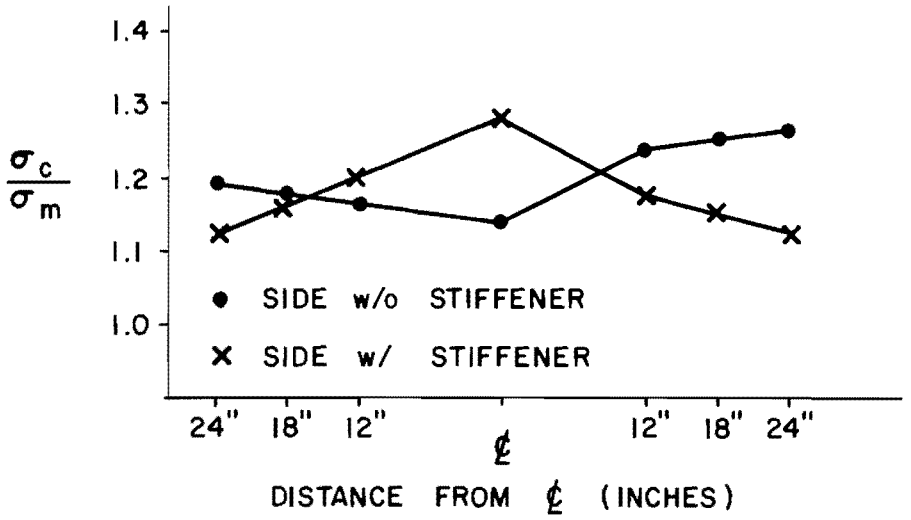

A) Top Flange

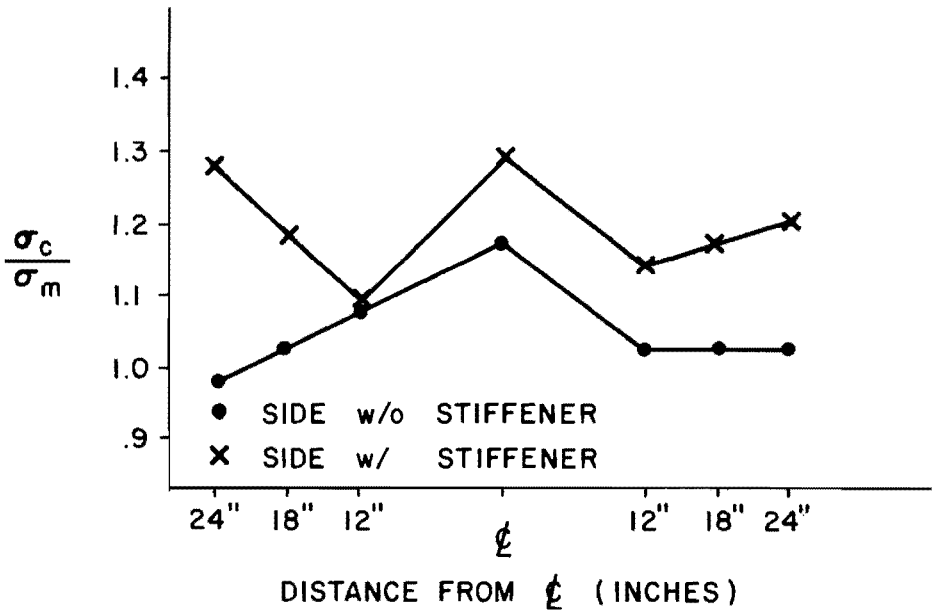

B) Bottom Flange

Fig. 4.8 Flange strain data for third static test P=37.4^{k}

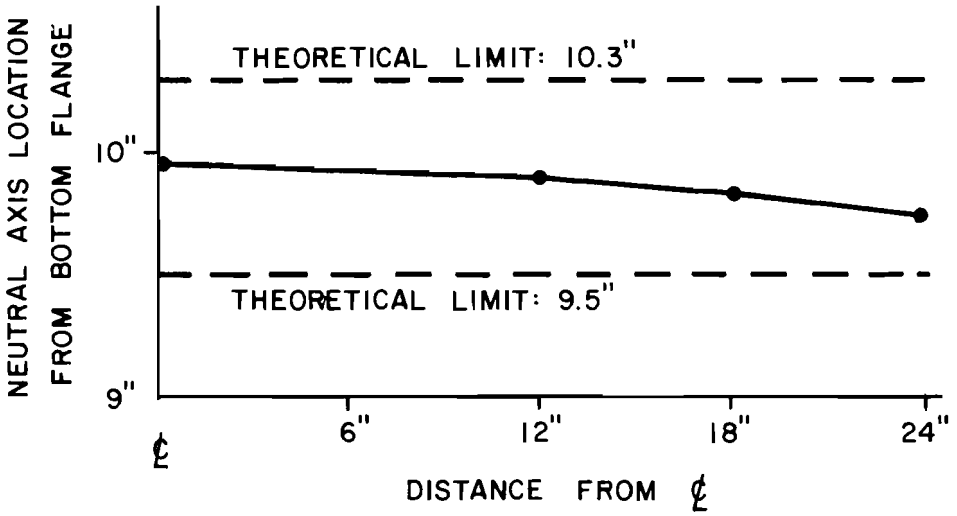

Fig. 4.9 Neutral axis location vs. distance from centerline, second static test

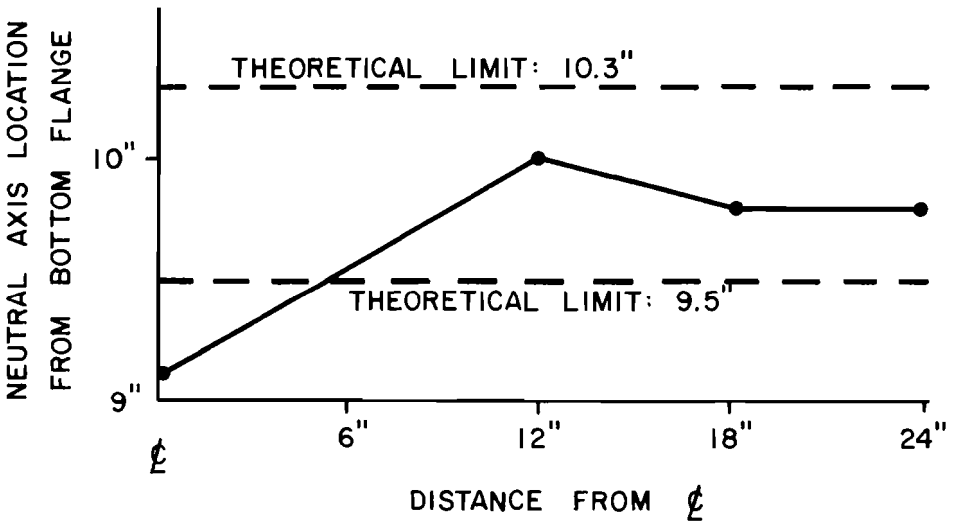

Fig. 4.10 Neutral axis location vs. distance from centerline, third static test

away from the centerline. Fig. 4.10 shows the same results using data from the third test with the tension flange braced.

The theoretical limits for the neutral axis is 10.3 inches, without the stiffener, and 9.5 inches with the stiffener. The results of these load tests show that the neutral axis is located at a value of around 9.7 - 10 inches from the bottom of the beam between 12 - 18 inches from the centerline. These results do not conclusively show that the location of the neutral axis has stabilized meaning that it is not known whether the longitudinal stiffener has become fully effective or not.

The stiffener gage results of the third test, shown in Table 4.3 gives a better idea as to what is happening. This data shows that the stiffener stress does not appreciably increase between 12 and 24 inches from the centerline. This indicates the stiffener has become fully effective in this length.

Analytical results show the stiffener becomes fully effective at a distance d, depth of the beam, from the end of the stiffener [6]. This is around 21 inches for the test specimen which corresponds to the results obtained in the second and third static tests.

With these results it can be concluded that the stiffener becomes fully effective within the constant moment region 30 inches to either side of the centerline.

4.4.4 Centerline Cross Sectional Behavior

It was not known how the cross section of the test specimen at the centerline behaved - whether as a stiffened or unstiffened section. All centerline calculations during the testing phase were performed using unstiffened section properties. If it was later determined that the cross section did not behave in this manner, the calculations could be altered.

The results of the second and third static tests indicate the neutral axis to be located between 9.1 inches and 10.4 inches above the bottom of the test specimen. The gages used for these calculations

Table 4.3 Average Stiffener Gage Results (μ-Strains) 3rd Static Test

LOAD (kips)	DISTANCE FROM CENTERLINE 12"	18"	24"
9.4	35	39	37
23.4	90	97	97
37.4	143	144	152
46.8	179	188	189

were the centerline gages shown in Fig. 3.9 and also the two top and two bottom flange gages at the centerline.

Again, the theoretical limits of the neutral axis location is between 10.3 inches and 9.5 inches above the bottom of the test specimen. These results indicate the same basic results shown in Fig. 4.10.

4.4.5 Neutral Axis Summary

The results of the previous two sections can be combined to get an overall picture of the neutral axis location. The neutral axis shifted slightly downward at the centerline, away from where it would be located if it were simply an unstiffened wide flange. There was no detectable neutral axis shift away from the centerline due to increased stiffener effectiveness. An exact location for the neutral axis cannot be determined using the data obtained in these tests. The tests do indicate that the neutral axis lies within the theoretical limits of 9.5 inches and 10.3 inches from the bottom of the beam.

4.4.6 Static Test Summary

Prior to the testing, there was difficulty in analyzing and predicting the behavior of the test section for several reasons. The section was unsymmetrical due to the longitudinal stiffener addition which caused a rotation of the principal axes and a shift in the location of the shear center. The rotation of the principal axes causes some out of plane movement of the test specimen under load. Because the beam is loaded in the plane of the web, the shift in shear center causes some out of plane movement and also causes torsion at the load points. When the test section is in the test frame, the bottom flanges are fixed against movement at the end reactions, there is some fixity at the load points due to the test specimen, and the top flanges at the ends of the beam are free to move. These conditions made it impossible to determine how the test section would react to load.

Since the longitudinal stiffener is discontinuous, it also causes changes in the location of the neutral axis and moment of inertia along its length.

Most of these problems would also occur on the actual bridge girder, however, their effects are magnified in the test section due to the difference in scale. It is not known how these problems effect the test results, however, it is believed that with the use of the braces, adverse effects due to torsion and out of plane bending could be held to a minimum. The results of the final static test on the top and bottom flange results fall within 10% of those calculated using elastic theory. This percentage of difference is considered acceptable due to the many problems and unknowns present and the results are considered representative of those that occur on the actual bridge girder.

4.5 Fatigue Test Results

Table 4.4 is a summary of the results of the fourteen dynamic tests that were run. Fig. 4.11 is the plot of these same results compared with the current Category Provisions in the AASHTO Bridge Specification. The stress range for the dynamic runs were calculated using the I_x of the stiffened section.

4.5.1 Non-Retrofit Specimens

All but one of the test specimens failed in one of two ways: with one crack or two. Figs. 4.12 and 4.13 show the typical failure patterns from the side of the web opposite the stiffener. By failed it is meant that a crack had grown through the web and was visible to the naked eye. All cracks originated at the toe of the weld at the end of the longitudinal stiffener in the stiffener intersection gap. There was no actual physical failure involved except for specimen #3 which cracked in half from about mid depth through the tension flange, Fig. 4.14. Once the specimen was cut open, Fig. 4.15, two separate initiation points were found: one at the toe of the weld at the end of the longitudinal stiffener and one at the toe of the tack weld at the base of the transverse stiffener. These had grown separately and caused a very sudden failure once they joined. This phenomena did not occur during either the first or second fatigue tests; however, it

Table 4.4 Fatigue Test Summary

DYNAMIC TEST	HEAT	GAP SIZE (")	S_R (ksi)	# OF CYCLES	CYCLES PER MINUTE	E' LIFE x 10^6 (cycles)	E LIFE x 10^6 (cycles)	A_{st}/t_w (AVG)
1	1	1/2	8	1,038,530	250	.7	1.9	4.92
2	1	1/2	5.2	2,101,230	500	2.8	7.	5.11
3	1	1/2	5.2	3,628,330	550	2.8	7.	5.17
4	2	1/2	5.2	1,349,770	550	2.8	7.	6.27
5	2	1/2	8	774,290	330	.7	1.9	6.13
6	2	2	8	847,240	360	.7	1.9	6.40
7	2	2	5.2	1,628,160	550	2.8	7.	6.32
8	2	1/2	3.2	5,781,800	600	14.	INFINITE	6.50
9	2	1/2	2.4	11,990,620	520	INFINITE	INFINITE	6.28
10	2	2	3.2	6,285,170	520	14.	INFINITE	6.47
11	2	1/2*	5.2	8,305,540	520	2.8	7.	6.21
12	2	1/2*	8	1,782,170	460	.7	1.9	6.5
13	2	1/2*	5.2	10,041,630**	520	2.8	7.	6.19
14	1	1/2*	8	3,189,420	350	.7	1.9	4.6

* Note: Stiffener intersection gap on these specimens were modified from 1/2" to 2" prior to testing.

** Specimen did not fail.

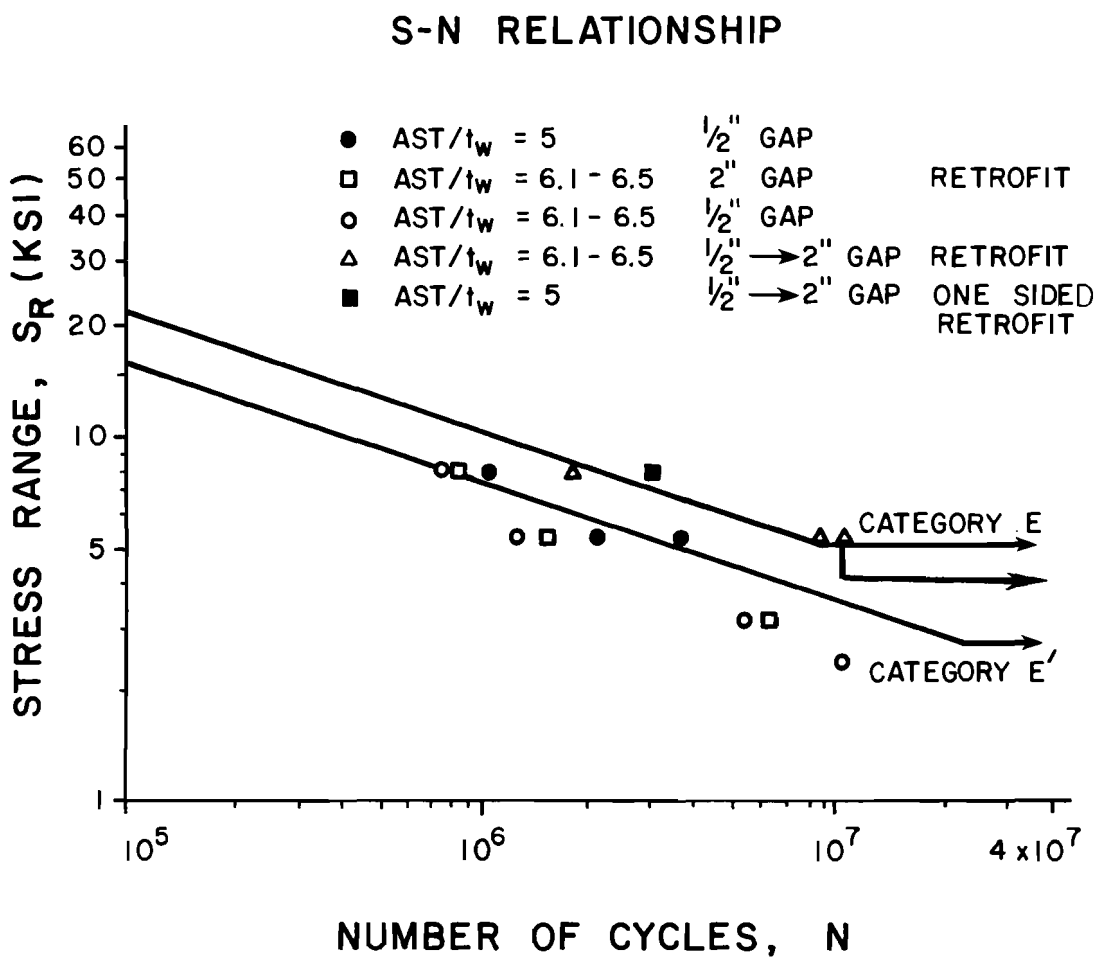

Fig. 4.11 Plot of fatigue test results

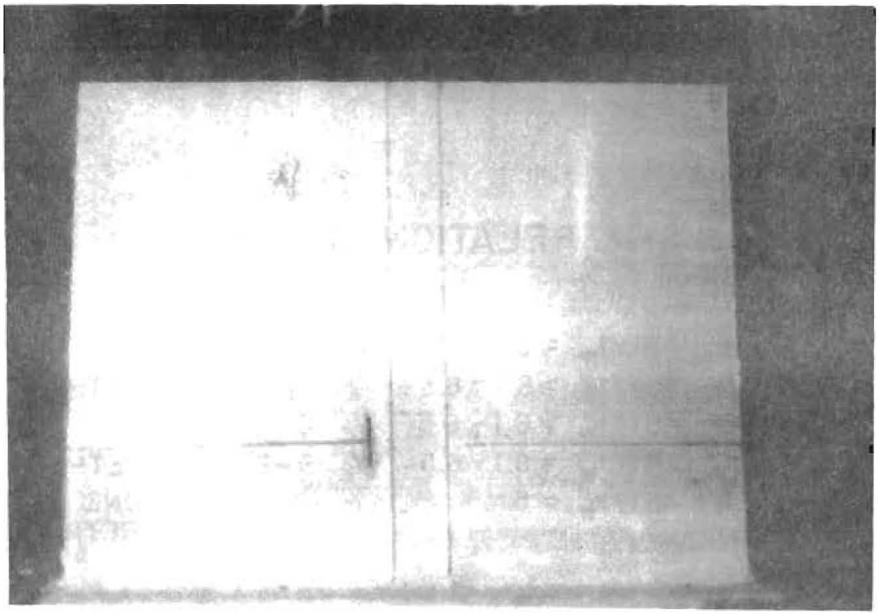

Fig. 4.12 Single crack in specimen

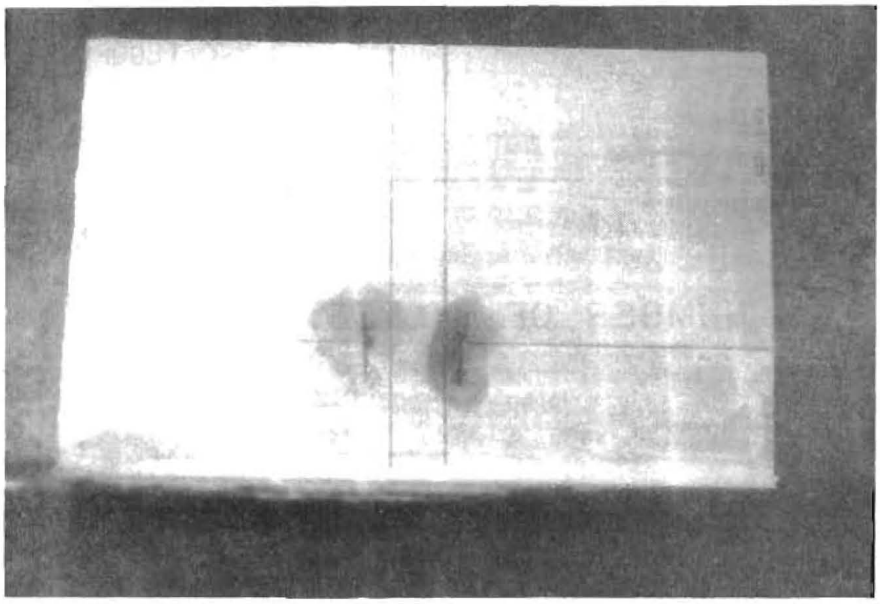

Fig. 4.13 Double crack in specimen

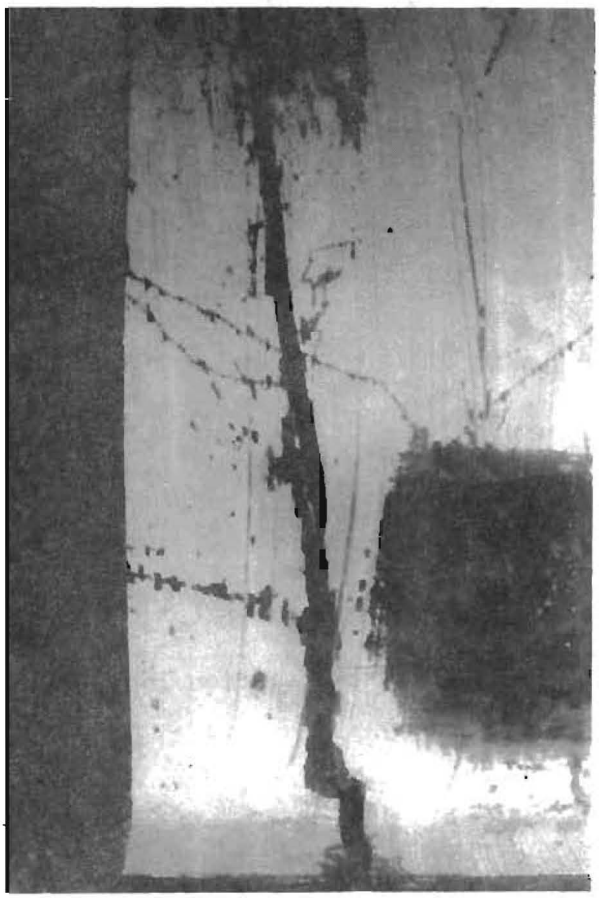

Fig. 4.14 Crack in dynamic specimen #3

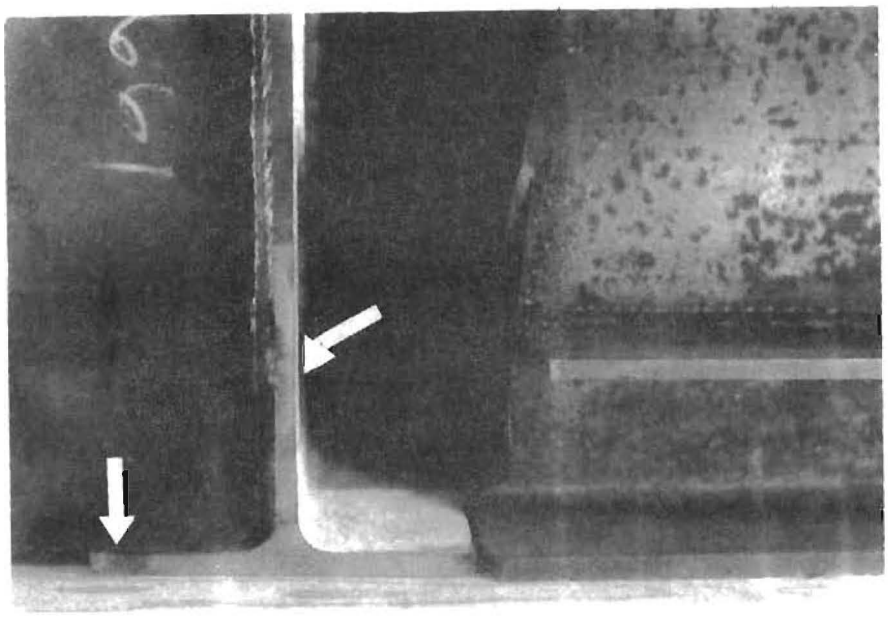

* Note: Arrows point to crack initiation location.

Fig. 4.15 Specimen #3 cut open showing crack initiation points

prompted the removal of the transverse stiffener tack weld for the remaining ten dynamic specimens.

4.5.2 Retrofit Specimens

There were two basic retrofit designs; one with a 2" gap detail and one with a plate welded to the transverse and longitudinal stiffener. The 2" gap detail failed in the same manner as the non-retrofit specimens - with one or two web cracks as shown in Figs. 4.12 and 4.13. The plate retrofit failed in a different manner. A crack initiated at the weld toe at the end of the outside weld joining the plate and the longitudinal stiffener as seen in Fig. 4.16, a Category E detail. The crack propagated towards the web sometimes completely cracking the plate in half. Once the crack had decreased the stiffness of the plate sufficiently, a crack then initiated (as in non-retrofitted specimens) at the toe of the weld in the gap at the termination of the longitudinal stiffener and formed the same type of web cracks shown in Figs. 4.12 and 4.13.

In the modified (one sided) retrofit specimen, shown in Fig. 2.7, the method of failure, seen in Fig. 4.17, was for the crack to form along the weld toe of the transverse stiffener on the side opposite the longitudinal stiffener. This is caused by the transverse stiffener being pulled in the direction of the attached longitudinal stiffener since it is not restrained on the opposite side.

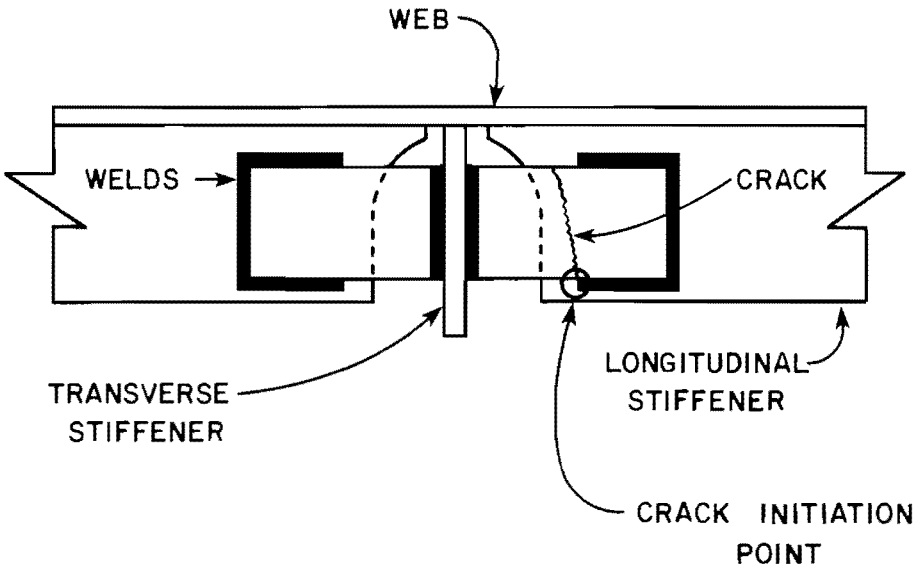

Fig. 4.16 Crack growth in continuous stiffener retrofit method

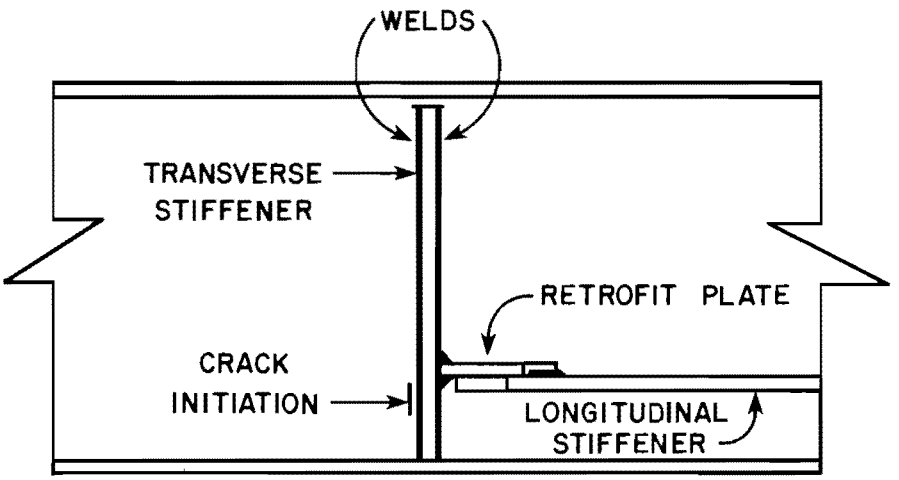

Fig. 4.17 Crack initiation in one-sided retrofit specimen

CHAPTER 5

EVALUATION OF FATIGUE TEST RESULTS

5.1 Introduction

The fatigue specimen results are discussed in this chapter with respect to the main variables involved: A_{st}/t_w, applied S_R, and retrofit method including gap size at the stiffener intersection.

5.2 Stress Range

The nominal stress can be computed using My/I_x, however, y and I_x are non-exact quantities. The two terms depend upon whether the section behaves as a stiffened or unstiffened section. The static tests performed on the cross section did not give conclusive results.

There is a difference of 20% when computing the stress range, S_R, at the location of the longitudinal stiffener termination using the two bounds (stiffened and unstiffened). For example, a S_R at the stiffener intersection of 10^{ksi} using an unstiffened cross section becomes 8^{ksi} using a stiffened cross section. This difference in S_R results in a design life of 1×10^6 cycles for the unstiffened section and 1.9×10^6 cycles for the stiffened section for a Category E detail, a 90% increase.

This presents a problem because the results with the second retrofit method (making the longitudinal stiffener continuous) which, due to its design produces a stiffened section, must be compared to the 1/2" and 2" gap details in order to evaluate the increased fatigue life due to the retrofit. A conservative approached will be utilized by using the stiffened cross section for computing the stress ranges. This not only allows the data to be compared with the second retrofit method results directly, it also results in a lower bound estimate of the fatigue life.

Table 5.1 Fatigue Test Results on Non-Retrofit Specimens

TEST #	GAP SIZE (INCHES)	UNSTIFFENED CROSS SECTION S_R (ksi)	STIFFENED CROSS SECTION S_R (ksi)	A_{st}/t_w RATIO	FATIGUE LIFE (cycles)
1	1/2	10ksi	8ksi	4.92	1,038,530
2	1/2	6.6	5.2	5.11	2,101,230
3	1/2	6.6	5.2	5.17	3,628,330
4	1/2	6.6	5.2	6.27	1,349,770
5	1/2	10	8	6.13	774,290
8	1/2	4	3.2	6.5	5,781,800
9	1/2	3	2.4	6.28	11,990,620

5.3 Ratio of A_{st}/t_w

Table 5.1 summarizes the results of the seven non-retrofit fatigue tests which are used to determine the effects of the A_{st}/t_w ratio on the fatigue life. The first three tests had a gap size of 1/2" and an A_{st}/t_w ratio of 5, they are plotted on Fig. 5.1. All three tests produced fatigue lives longer than Platten's prediction. but less than the fatigue life of a Category E.

The next four tests run with a 1/2" gap (tests #4, #5, #8, #9) had an A_{st}/t_w ratio between 6.1 and 6.5 with all other dimensions the same as the three previous specimens. The results of these tests are also plotted on Fig. 5.1. The results at a S_R of 8^{ksi} and 5.2^{ksi} show that the larger area of stiffener reduced the fatigue life. This agrees with the trend shown for the stress concentrations shown in Fig. 1.5.

For tests #8 and #9 there is no test at a comparative S_R with the A_{st}/t_w ratio of 5. The failure of these specimens at the low stress ranges indicates the poor performance of the detail.

This corresponds with the results of Platten's analysis which predicted that the larger the A_{st}/t_w ratio, the shorter the fatigue life of the detail. All four of the tests produced fatigue lives longer than Platten's estimate but shorter than the normal design Category E fatigue life. Since none of the specimens tested had an A_{st}/t_w ratio of 7 as analyzed by Platten, it is not entirely accurate to directly compare the results. However, the results obtained indicate a fairly close correlation between theory and experimental data.

5.4 Retrofit Results

This section presents the results of tests #6, #7, #10, #11, #12, #13 and #14. Tests #11-#14 were retrofits with the plate welded to both the transverse and longitudinal stiffener with the remainder being the 2" gap retrofit specimens. Table 5.2 presents a summary of the retrofit specimen results.

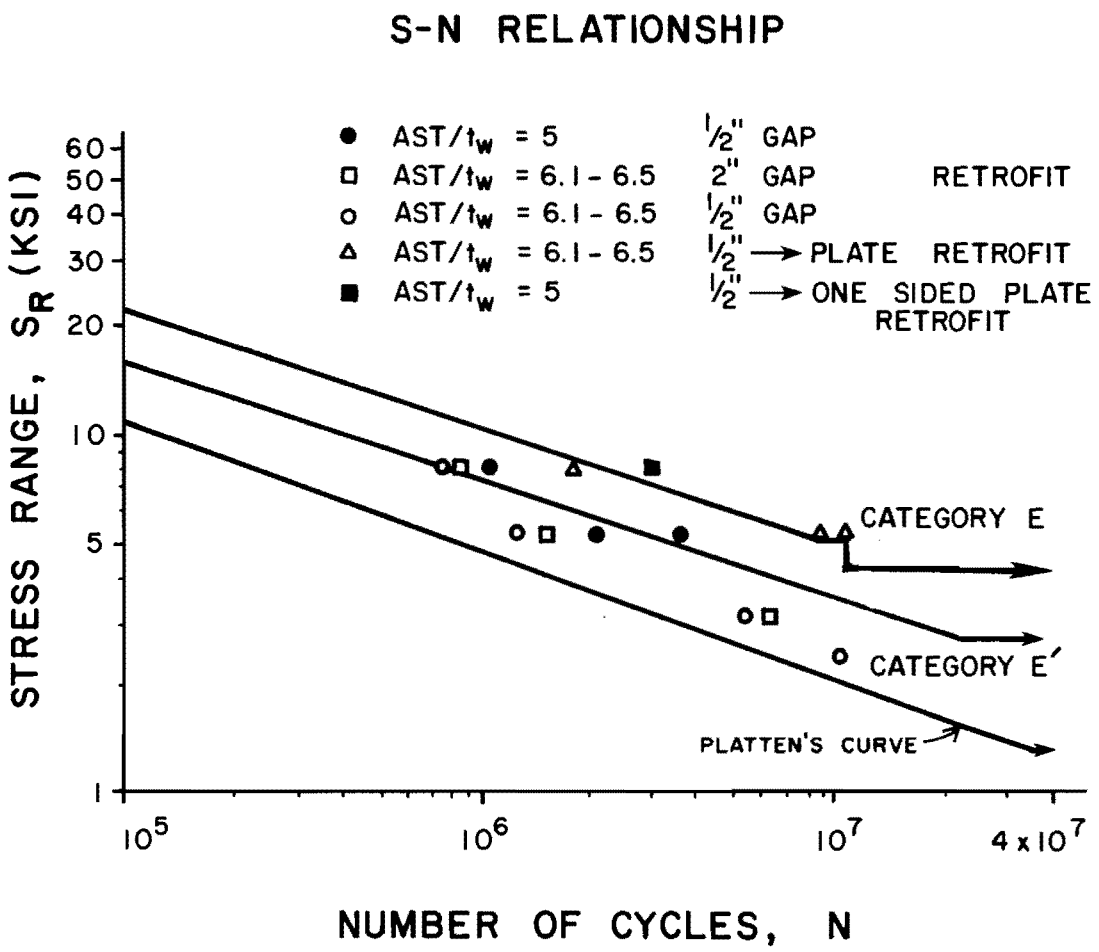

Fig. 5.1 Fatigue test results

Table 5.2 Fatigue Test Results on Retrofit Specimens

TEST #	GAP SIZE (INCHES)	UNSTIFFENED CROSS SECTION S_R (ksi)	STIFFENED CROSS SECTION S_R (ksi)	A_{st}/t_w RATIO	FATIGUE LIFE (cycles)
6	2	10ksi	8ksi	6.4	847,620
7	2	6.6	5.2	6.32	1,628,160
10	2	4	3.2	6.47	6,285,170
11	1/2	6.6	5.2	6.21	8,305,540
12	1/2	10	8	6.5	1,782,170
13	1/2	6.6	5.2	6.19	10,030,000*
14	1/2	10	8	4.6	3,189,420

* NOTE - Specimen 13 did not fail. See text Chap. 5.4.2

5.4.1 Influence of Gap Size

Tests #6, #7 and #10 were conducted with the same A_{st}/t_w ratio as the previous four tests #4, #5, #8 and #9, A_{st}/t_w ratio of 6.1-6.5, with the difference in the specimens being the gap between the longitudinal and transverse stiffeners. In tests #6, #7 and #10 the gap was increased to 2" from the previous 1/2". The results are plotted in Fig. 5.1. All three specimens can be compared directly with tests performed at similar stress ranges and the same A_{st}/t_w ratio. In all three cases, an increased gap length produced an increase in fatigue life, however, the increase is not as dramatic as that predicted by Platten's analysis.

If the increased gap results are compared against those of the smaller A_{st}/t_w ratio with the 1/2" gap, it shows that an increase in gap length does not produce the same fatigue life increase as the reduced A_{st}/t_w ratio.

5.4.2 Influence of Retrofit Plates

Tests #11, #12 and #13 were conducted with an A_{st}/t_w of between 6.1 and 6.5. Plates were welded joining the transverse and longitudinal stiffeners, shown in Fig. 2.6. Prior to welding plates on specimen #13, the specimen was subjected to 250,000 cycles. This was to simulate the number of cycles presently on the actual bridge girders to see if previous damage due to fatigue loading would shorten the retrofitted fatigue life of the specimen. The results of these three tests are plotted in Fig. 5.1.

In comparing the results at both 8^{ksi} and 10^{ksi}, the retrofit method of welding a plate to both longitudinal and transverse stiffeners shows a relatively large increase in the fatigue life over all the previous specimens. The results of specimens #11 and #13 show that previous fatigue loading history (which in this case approximated 20% of the design life of the structure) did not shorten the fatigue life of the specimen. Test #13 was terminated after it reached the fatigue life of specimen #11, it did not fail.

The purpose in joining the transverse and longitudinal stiffeners by a welded plate was to attempt to make the longitudinal stiffener continuous over the length of the beam -- a Category B detail. However, in the process of joining the plates, some Category C and E details were produced due to the location of the stiffener to plate welds. The weld between the transverse stiffener and the retrofit plate is a Category C detail while the termination of the welds joining the retrofit plate to the longitudinal stiffener is a Category E detail. The end results indicate that the fatigue life of the original detail - A_{st}/t_w ratio of 6.5-6.1 and a 1/2" gap - was increased to a Category E weld detail by the addition of the plates joining the longitudinal and transverse stiffener.

The comparison of tests #11 and #13 indicate that even though a specimen may have been subjected to fatigue loading representing a significant portion of its intended design life, the addition of the retrofit plates still increased the fatigue life. The test result indicates no decrease in life expectancy due to previous cyclic loading.

5.4.3 Influence of One Sided Longitudinal Stiffener

Extensive testing was not performed on this detail. One test was performed to determine if the one sided detail would produce fatigue life comparable to the two sided detail.

Test #14 was conducted with a one sided longitudinal stiffener and retrofit, an A_{st}/t_w ratio of 4.6 and a S_R of 8ksi. A modification was made to the retrofit plate to prevent the type of failure occurring in tests #11, #12 and #13. Fig. 4.16 shows the crack initiation point at the end of the fillet weld for these three test specimens modified with the plate retrofit. Fig. 2.7 shows the shape of the modified plate. The modifications were done in order to reduce the stress concentration at the fillet weld.

The results of this test is plotted on Fig. 5.1. It indicates that a one sided retrofit specimen can expect a longer fatigue life than a comparable two sided retrofit specimen. The modification performed to the retrofit plate has increased the fatigue life of the

retrofit plate weld detail such that the crack initiation point has moved back into the web at the stiffener intersection as seen in Fig. 4.17.

CHAPTER 6

SUMMARY

6.1 Stiffener Intersection Detail Fatigue Performance

The experimental study consisted of 14 fatigue tests performed on steel wide flange sections with various geometries of longitudinal-transverse stiffener intersections. Two geometries were used to determine the influence of the ratio of A_{st}/t_w on the fatigue life of the particular detail. Several modifications of the stiffener intersection detail to increase its fatigue life were also investigated. The results of these experimental tests were then compared with an analytical study and the following conclusions drawn.

6.1.1 Conclusions

1) The fatigue life of the stiffener intersection detail was shorter than the design fatigue categories E and E' in the AASHTO specification.

2) As the ratio of the stiffener area to web thickness (A_{st}/t_w) increased, the fatigue life decreased.

3) An increase in gap size between the longitudinal and transverse stiffener from 1/2" to 2" increased the fatigue life.

4) Retrofitting the longitudinal stiffener by welding a plate between it and the transverse stiffener increased the fatigue life to Category E.

5) A one sided retrofit showed an increased fatigue life over the typical unmodified two sided stiffener intersection detail.

6) A specimen subjected to 20% of its intended design life before being retrofit showed an increase in its fatigue life.

7) The finite element study results compared favorably with the experimental results.

6.1.2 Recommendations for Design

The results of the tests in this study indicate that there is a large variance in the fatigue life of the particular weld detail

under study dependent upon its geometry. The fatigue design curves in the AASHTO Specifications do not cover the stiffener detail investigated. The following is offered as recommendations in the fatigue design of stiffener intersections:

1) avoid stiffener intersections if possible
2) attach the longitudinal stiffener to transverse stiffeners using a partial penetration fillet weld designed according to the procedure in Appendix B, section B.3.

6.2 Expected Fatigue Performance of Bridge Studied

The results of this project indicate that the critical detail on this bridge is the stiffener intersection. The estimated fatigue life is between 45 and 80 years. The other details investigated on the bridge do not appear to be prone to fatigue crack growth due to a combination of the low measured stresses and the good fatigue performance of the details.

It is recommended that the retrofit procedure given in Appendix B be applied to the longitudinal stiffeners in the web panels at the location of the dead load moment inflection point. It is also recommended that other bridges with similar details also be retrofitted.

A P P E N D I X A

NOTATIONS

N O T A T I O N

A_f - Area of compression flange (in^2)

A_{st} - Cross-sectional area of stiffener (in^2)

b_s - Width of longitudinal stiffener (in)

d - Overall depth of beam (in)

I - Moment of inertia of a section (in^4)

K_t - Stress concentration factor

M - Bending moment (kip-ft)

N - Cyclic frequency - number of cycles

S_R - Stress range (ksi)

t_s - Longitudinal stiffener plate thickness (in)

t_w - Web thickness (in)

x - Subscript relating symbol to strong axis bending

y - Subscript relating symbol to weak axis bending

y - Distance from centroid of section to extreme fiber in bending (in)

A P P E N D I X B

RETROFIT PROCEDURE

RETROFIT PROCEDURE

The retrofit procedure detailed below is recommended for implementation on the bridge investigated in this study and other bridges with similar stiffener intersection details. The retrofit should be applied to the stiffener intersections on each side of the dead load inflection point. Figure 2.6, page 20, shows the recommended retrofit detail. A similar detail can be used if a longitudinal stiffener is on one side of the transverse stiffener.

B.1 Retrofit Plate Design

The plate to be welded to the longitudinal stiffener and the transverse stiffener should have a cross-sectional area equal to that of the longitudinal stiffener. The retrofit plate width should be less than the longitudinal stiffener width to allow clearance for the fillet welds attaching the retrofit plate to the longitudinal stiffener.

B.2 Retrofit Plate to Longitudinal Stiffener Fillet Weld

This fillet weld should have a design strength equal to the design allowable strength of the longitudinal stiffener (design allowable strength = $0.55\ F_y \times A_{st}$).

B.3 Retrofit Plate to Transverse Stiffener Weld

In order to provide that premature cracking does not occur from the weld root, a two-sided partial penetration weld is required. The required weld size is a function of the retrofit plate thickness. The equation for the required weld size is:

$$0.79\ H + 2.60\ P = t_p\ (1.10\ t_p^{1/6} + 0.69)$$

where H = fillet weld leg size, in.;

P = depth of penetration, in.; and

t_p = thickness of retrofit plate, in.

The weld should also have a capacity equal to the design allowable tension of the longitudinal stiffener.

B I B L I O G R A P H Y

1. Fisher, J. W., Albrecht, P. A., Yen, B. T., Klingerman, D. J., and McNamee, B. M., "Fatigue Strength of Steel Beams with Transverse Stiffeners and Attachments," NCHRP Report #147, Highway Research Board, 1974.

2. Fisher, J. W., Frank, K. H., Hirt, M. A., and McNamee, B. M., "Effect of Weldments on the Fatigue Strength of Steel Beams," NCHRP Report #102, Highway Research Board, 1970.

3. AASHTO Subcommittee on Bridges and Structures, Standard Specifications for Highway Bridges, American Association of State Highway and Transportation Officials, Twelfth Edition, Washington, D.C., 1977.

4. AASHTO Subcommittee on Bridges and Structures, Interim Specifications, Bridges, 1979 American Association of State Highway and Transportation Officials, Washington, D.C., 1979.

5. Fisher, J. W., Hausammann, H., Sullivan, M. D., and Pense, A. W., "Detection and Repair of Fatigue Damage in Welded Highway Bridges," NCHRP Report #206, Highway Research Board, 1979.

6. Platten, D. A., "Analytical Study of the Fatigue Behavior of a Longitudinal - Transverse Stiffener Intersection," unpublished M.S. thesis, University of Texas at Austin, May 1980.

7. Gupta, A., "Field Tests of a Continuous Twin Girder Steel Bridge," unpublished M.S. thesis, University of Texas at Austin, May 1980.

8. Fisher, J. W. and Frank, K. H., "Fatigue Strength of Fillet Welded Cruciform Joints," Journal of the Structural Division, ASCE, Vol. 105, No. ST9, September 1979, pp. 1727 - 1740.